WEAK INTERACTIONS OF QUARKONIA*

By J. H. Kühn

Max-Planck-Institut für Physik und Astrophysik, Munich**

(Received October 18, 1980)

The following topics are discussed in this article: parity violating effects in $e^+e^- \to 1^{--}$ resonance and the subsequent leptonic decay, the formation of 1^{++} resonances in e^+e^- annihilation, weak decays of superheavy-onia ($M = 40-150$ GeV), Z_0 decays into- onia and photons or Higgs particles, parity mixing of -onium levels, the relative branching ratios for various charmonium channels in B-meson decays, neutrino production of charmonium.

PACS numbers: 13.10.+q

Table of Content

I. Introduction
II. Parity Violation on a 1^{--} Resonance
1. General Remarks
2. Longitudinally Polarized Beams
3. Analysis of $\tau^+\tau^-$ Final States
III. Neutral Current Formation of Axial Resonances
1. Cross Section and Parity Violation
2. Wave Function Estimates
3. Electromagnetic Backgrounds: $e^+e^- \to \gamma^*\gamma^* \to 1^{++}$
IV. Superheavy Resonances
1. General Remarks
2. Quarkonia in Z_0 Decays
3. Weak Decays of Superheavy Quarkonia
a) Annihilation Decays
b) Single Quark Decays
V. Parity Mixing
1. General Remarks
2. The Mixing Angles
3. The Decay $2^3S_1 \to 1^3S_1 + \gamma$
VI. Charmonium in B-Decays

---

* Extended version of lectures presented at the XX Cracow School of Theoretical Physics, Zakopane, May 29 — June 11, 1980.

** Address: Max-Planck-Institute für Physik und Astrophysik, Föhringer Ring 6, 8000 München 40, West Germany.

VII. Neutrino Production of Charmonium
1. General Remarks
2. Photo and Muo Production of ψ
3. Neutrino Production
4. Other Charmonium States

1. INTRODUCTION

The physics of quarkonia — mesons which are understood as nonrelativistic bound-states of a heavy quark and antiquark [1] — has contributed a lot to our understanding of hadron physics. The forces between quarks at intermediate distances have been determined through the analysis of energy levels, radiative transitions and leptonic decays. Strong decays are short distance processes and thus have been successfully evaluated in perturbative QCD [2–4]. Many results for charmonium still suffer from unknown and uncontrollable corrections like relativistic effects, ambiguities in the choice of the potential, higher order QCD corrections and limited phase space. However, for heavier systems like the Υ and the presumed toponium many of the standard results should be far more reliable and will lead to rather stringent tests of the model.

Heavy onia may well have masses, where weak, electromagnetic and strong interactions are of comparable strength. Then they could serve to measure otherwise hardly accessible couplings like the neutral current coupling to heavy quarks [5–7].

The decays and transition rates involve necessarily wave functions which we shall express through other observables as far as possible. Extensive potential model calculations are beyond the scope of this lecture. Whenever absolute rates are calculated for fictitious heavy onia using simple potentials, they only illustrate the order of magnitude and are not meant as absolute predictions.

I shall be concerned mostly with the interactions of heavy quarks alone. Only in the last chapter I shall treat production of charmonium in neutrino reactions and in B-decays, and only in this case the interaction of heavy quarks with ordinary hadrons comes into play.

The lecture will be organized as follows: In Chapter II I shall discuss parity violating effects in the reaction $e^+e^- \to 1^{--}$ resonance and the subsequent leptonic decay. The formation of 1^{++} resonances in e^+e^- annihilation will be treated in Chapter III. Weak decays of superheavy onia (M = 40–150 GeV) might be accessible at LEP and will be considered in Chapter IV. This part contains hitherto unpublished results. The techniques are closely related to the evaluation of Z_0 decays into onia and photons or Higgs particles, and therefore all these reactions will be treated in parallel. In Chapter V I shall give new unpublished results on parity mixing of onium levels and their implication on the C violating decay of the first radially excited level 2^3S_1 into the ground-state 1^3S_1 and a photon. It has been proposed that the decay of B mesons into $\psi K\pi$ might be one of the few exclusive channels which can be observed. In Chapter VI the relative branching ratios for the various charmonium channels are calculated. Chapter VII finally is concerned with neutrino production of charmonium. I shall compare the predictions of a specific QCD model, based on "local duality" with the predictions of the vector dominance model and shall contrast their results and their region of applicability.

II. PARITY VIOLATION ON A 1^{--} RESONANCE

II.1. General considerations

Perhaps the most important step after the detection of a new flavor is to determine whether the new quarks fit again into the repeatedly successful scheme of weak isodoublet generations. The quark charge is measured most easily in e^+e^- annihilation through a step in R or through the electronic width of the lowest lying $^3S_1$ state[1].

The weak coupling to the charged current can be determined through the weak decays of the new flavored mesons ($Q\bar{q}$). The neutral current coupling however requires the interaction of Q and $\bar{Q}$ and therefore onia are the right systems to investigate.

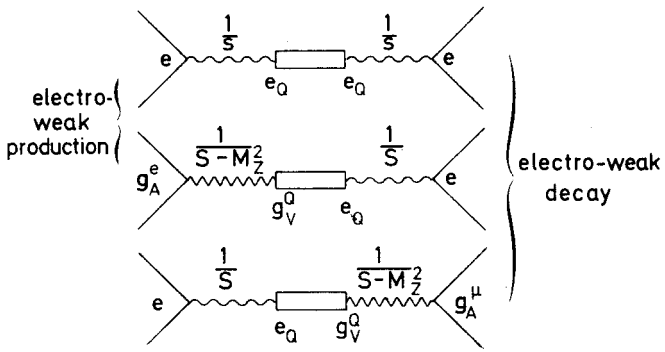

Fig. II.1

As a first example I shall discuss parity violation in the production and decay of a ψ-like heavy resonance[2]. A resonance with the quantum numbers 1^{--} can be produced from the vacuum through the electromagnetic current and through the vector part of the neutral current. For masses well below M_Z all rates will be completely dominated by the electromagnetic interaction. Only the parity violating interference of weak and electromagnetic amplitudes will lead to observable effects either in the production or in the decay of the 1^{--}.

To measure parity violation we have to measure psuedoscalars like $\vec{\sigma}\vec{p}$ or $\vec{p}_1 \times \vec{p}_2 \cdot \vec{p}_3$. The second one is trivially zero for the $\mu^+\mu^-$ final state due to momentum conservation. However, also for the multihadron decay lowest order QCD calculations give a vanishing result. Any T odd quantity could be different from zero only in the presence of large final state interactions or a large absorptive part of the amplitude [4]. We therefore concentrate on T-even pseudoscalars like $\vec{\sigma}\vec{p}$. We either fix the spin of the incoming electrons and polarize the beam (Section II.2) or measure the spin of the decay products (Section II.3).

---

[1] The levels of the $Q\bar{Q}$ system will be labeled in spectroscopic notation by $^1S_0, ^3S_1, ^3P_0, ^3P_1, ^3P_2, \ldots$ or alternatively by their quantum numbers $J^{PC} = 0^{-+}, 1^{--}, 0^{++}, 1^{++}, 2^{++}$. Only if necessary, the ground state, eg., 1^1S_0 and the radial excitation 2^1S_0 will be discriminated.

[2] This has been discussed by Bigi, Kühn and Schneider [1] for polarized beams and by Koniuk, Leroux and Isgur [2] and by Budny [3] for unpolarized beams and leptonic decay modes.

One important point should be stressed: all these asymmetries involve only ratios of amplitudes, are independent of quarkonium dynamics and thus measure directly the weak couplings.

II.2. Longitudinally polarized beams[3]

The electro weak production amplitude is given by

$$\mathcal{M} = \bar{e}\gamma_\mu(1+r_e R\gamma_5)e\ 4\pi\alpha f_V \mathscr{E}_\mu, \tag{1}$$

where $\mathscr{E} \equiv$ polarization vector of 1^{--}, $M^2 f_V \mathscr{E}_\mu \equiv \langle 0|J_\mu^{EM}|1^{--}\rangle$, $r_e \equiv \dfrac{g_A^e g_V^Q}{e^2 \hat{e}_Q}$ = ratio of weak to electromagnetic couplings, $R \equiv \dfrac{M^2}{M^2 - M_z^2}$ = ratio of the propagators. The vector part of the leptonic neutral current leads only to a negligible change of the total cross section which will be neglected.

For the extreme case $r_e R = +1$ (-1) only right (left) handed electrons couple and the cross section is zero for the "wrong" polarization. In general the *parity violating asymmetry in the production cross section* for 100% polarization is

$$S \equiv \frac{\sigma_{RH} - \sigma_{LH}}{\sigma_{RH} + \sigma_{LH}} = \frac{2 r_e R}{1 + (r_e R)^2}. \tag{2}$$

Longitudinally polarized beams also lead to an alignment of the resonance spin and this allows us to observe a parity violating $\cos\theta$ term in the leptonic decay distribution (Fig. II.2) like in the original β decay experiment.

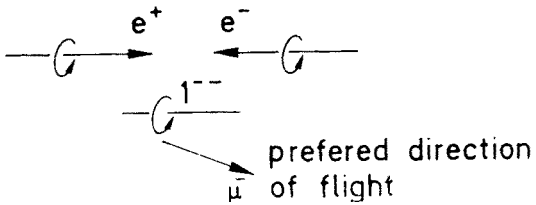

Fig. II.2

The integrated forward backward asymmetry

$$A_{FB} \equiv \frac{\displaystyle\int_0^1 d\cos\theta \frac{d\sigma}{d\cos\theta} - \int_{-1}^0 d\cos\theta \frac{d\sigma}{d\cos\theta}}{\displaystyle\int_{-1}^1 d\cos\theta \frac{d\sigma}{d\cos\theta}} = \frac{3}{2}\frac{r_\mu R}{1+(r_\mu R)^2} \tag{3}$$

[3] This section is mainly based on Ref. [1].

reverses its sign with the beam polarization. The absolute magnitude of S in the WS-model[4] for $\sin^2\theta_W = 0.23$ is given in Table I and $A_{FB} = 3/4\ S$ if we assume $r_e = r_\mu$.

With longitudinally polarized beams we thus have the possibility to measure $g_A^e g_V^Q$, and $g_A^\mu g_V^Q$, separately.

TABLE II.I

S in % for $\sin^2\theta_W = 0.23$

Mass (GeV)	9.5	35	45
$Q = 2/3$	×	7,3	10,0
$Q = -1/3$	1,65	25,8	35,2

II.3. Analysis of $\tau^+\tau^-$ final states

Even for unpolarized beams we may try to analyse the helicity of the μ- and τ-pairs through their weak decays. Particularly asymmetries in ψ-decays into leptons and hadrons have been analysed by Koniuk, Leroux and Isgur [2] and later also by others [3, 5]. The τ-net helicity

$$h(\theta) = -\frac{2R}{(1+\cos^2\theta)}\,(r_\tau(1+\cos^2\theta)+2r_e\cos\theta) \tag{4}$$

has a symmetric positive contribution from the weak decay, proportional to r_τ which leads to a distortion of the decay spectra. The antisymmetric contribution proportional to r_e is a result of the net polarization of the 1^{--} due to its electroweak production.

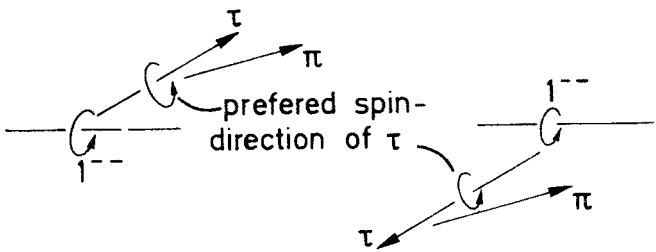

Fig. II.3

To be specific, let us consider the $\tau^- \to \pi^-\nu$ decay in more detail (Fig. II.3). $Rr_e > 0$ leads to a negative (positive) helicity of forward (backward) produced τ's. The pion is preferentially emmitted in the direction of the τ^- spin,

$$\frac{dN}{d\cos\theta} = \tfrac{1}{2}(1+\cos\theta), \tag{5}$$

[4] For the neutral current couplings of leptons and quarks see Appendix A.

(θ = angle between $\vec{p}_\pi$ and spin of τ in the rest frame) which is against (in) the direction of flight of the τ^- and therefore has a relatively small (large) fraction of the energy. The energy dependent angular distribution in the CM-frame is then given by

$$\frac{dN}{dX d\cos\theta} \propto 2(m_\tau^2 - m_\pi^2)(1+\cos^2\theta) + 8 r_e R (m_\pi^2 - m_\tau^2 X)\cos\theta \tag{6}$$

$$X \equiv \frac{E_\pi}{E_\tau}, \qquad E_\tau \gg m_\tau, \qquad E_\pi \gg m_\pi,$$

and leads to an energy dependent forward backward asymmetry.

$$A_{FB}(X) \equiv \frac{\int_0^1 d\cos\theta \frac{d\sigma}{d\cos\theta dX} - \int_{-1}^0 d\cos\theta \frac{d\sigma}{d\cos\theta dX}}{\int_{-1}^1 d\cos\theta \frac{d\sigma}{d\cos\theta dX}}$$

$$= -\frac{m_\pi^2 - m_\tau^2 X}{m_\pi^2 - m_\tau^2} \tfrac{3}{2} r_e R \approx -\tfrac{3}{2} r_e R X \tag{7}$$

in the π distribution[5]. Similar asymmetries have been analysed also for the leptonic decay modes [2, 3, 5].

III. FORMATION OF AXIAL RESONANCES[6]

III.1. Cross section and parity violation

In the last chapter we were looking for reactions, where neutral current effects could be detected through weak-electromagnetic interferences. Here I want to consider e^+e^- annihilation into final states which contain only particles with positive charge conjugation. This eliminates the one photon channel and leaves us with neutral current reactions. (Higher order QED could also contribute and will be considered in Section III.3). Multiparticle final states consisting e.g. of π^0 and η give negligible rates: weak effects are small at low energies and final states with π^0 and η only are rare at high energies. Furthermore such channels could be faked through weak decays.

There is however the possibility of resonant formation of $^3P_1$ quarkonium with the quantum numbers $J^{PC} = 1^{++}$. The cross section is not suppressed by any formfactor and — since we deal with a narrow resonance — even enhanced for $E_{CM} = M_{1++}$. The reaction measures the axial coupling of heavy quarks together with some wave function dependent onium dynamics.

---

[5] The same result holds for the $\tau \to \rho\nu$ decay.

[6] This part is based on work done in collaboration with J. Kaplan [1].

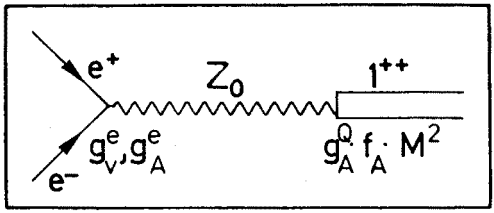

Fig. III.1

Firstly I shall derive the formulas for the cross section and the parity violation. In Section III.2 I shall discuss the mass dependence of the cross section, using specific results of potential models. Electromagnetic background reactions will be treated in Section III.3

The production amplitude

$$\mathcal{M} = \bar{e}\gamma_\mu(g_V^e + g_A^e\gamma_5)e \frac{1}{M^2 - M_Z^2} g_A^Q M^2 f_A \mathcal{E}^\mu \tag{1}$$

with

$$g_A^Q M^2 f_A \mathcal{E}^\mu \equiv \langle 0|g_A^Q A^\mu|1^{++}\rangle \tag{2}$$

involves vector and axial couplings at the electron vertex, but only the axial coupling of heavy quarks at the hadronic vertex. Let me briefly mention some of the qualitative features of the reaction. Since it is an entirely weak process, one expects a sizeable parity violation. Even for unpolarized beams the resonance's spin is aligned with the beam direction

$$\langle \vec{S} \cdot \vec{p}_e/|p_e|\rangle = \frac{2g_V^e g_A^e}{g_V^{e2} + g_A^{e2}} . \tag{3}$$

This polarization is however difficult to detect in electromagnetic and strong decays. For longitudinally polarized beams one finds furthermore a difference in the cross section

$$\frac{\sigma_{RH} - \sigma_{LH}}{\sigma_{RH} + \sigma_{LH}} = \frac{2g_V^e g_A^e}{g_V^{e2} + g_A^{e2}} . \tag{4}$$

In general this is of order one, however, due to the specific value of the Weinberg angle $\sin^2\theta_W \approx 1/4$, it is numerically small.

In contrast to the previous chapter, however, we do not have to rely on parity violation to identify the effect of the neutral current. A resonating cross section at the correct energy would already prove the presence of a P and C violating coupling.

For a narrow resonance it is customary to express the integrated cross section through the electronic width

$$\int dE\sigma(E) = 6\pi^2\Gamma_{e^+e^-}/M^2 \tag{5}$$

which is given by

$$\Gamma_{e^+e^-} = \frac{g_A^{e2}+g_V^{e2}}{12\pi} f_A^2 \frac{M^5}{(M^2-M_Z^2)^2}$$

$$= \frac{G_F^2 M^5}{96\pi} f_A^2(1+(1-4\sin^2\theta_W)^2) \frac{1}{(1-(M/M_Z)^2)^2}. \tag{6}$$

The measured cross section on top of the resonance depends further on the energy spread[7] ΔE_{CM}

$$\sigma_{top} = \frac{6\pi^2 \Gamma_{e^+e^-}}{M^2\sqrt{2\pi}\,\Delta E_{CM}}. \tag{7}$$

The nonrelativistic onium model is now used to evaluate the axial vector coupling. For P-state production and decay only $R_P'(0)$, the derivative of the wave function at the origin contributes. The amplitude is given in terms of the wave function $\psi_{s\bar{s}}(\vec{k})$ by

$$A = 1/\sqrt{m} \int \frac{d\vec{q}}{(2\pi)^{3/2}} \psi_{s\bar{s}}(\vec{q})\, \bar{v}(\bar{Q}, s)\gamma_\mu\gamma_5 u(Q, s),$$

$$Q-\bar{Q} = (0, 2\vec{q}), \quad Q+\bar{Q} = (M, 0), \quad 2m = M,$$

$$\sum_{s\bar{s}} \int d\vec{q} |\psi_{s\bar{s}}(\vec{q})|^2 = 1. \tag{8}$$

With the techniques described in Appendix B one obtains[8]

$$f_A^2 = \frac{9}{4\pi}\frac{1}{m^5}|R_P'(0)|^2 \tag{9}$$

which should be contrasted with the corresponding vector coupling

$$f_V^2 = \frac{3}{8\pi}\frac{1}{m^3}|R_P(0)|^2. \tag{10}$$

In the chiral limit one expects $f_V = f_A$, in the nonrelativistic limit on the other hand $f_A/f_V \to 0$, since f_A involves another factor q/m. To give numerical results for the f's and the wave functions one has to use some more or less realistic potential models. Since $|R_S(0)|^2$ and $|R_P'(0)|^2$ enter all S- and P-wave production and decay rates, their mass dependence will be treated in more detail in the next section.

---

[7] Radiative corrections, which reduce σ_{top} by several tens of percent, are neglected.

[8] Color is taken into account.

III.2. Wave function estimates

As stated already above, f_A^2/f_V^2 is of order $q^2/m^2 = (v/c)^2$ in the nonrelativistic limit. Therefore we expect that this ratio decreases for increasingly heavy onia. This expectation is supported by the scaling behaviour [I.3] for a power law potential $V(r) = \lambda r^\nu$. Lengths scale like $L \propto (\mu|\lambda|)^{-1/(2+\nu)}$, energy differences like $\Delta M \propto \mu^{-\nu/(2+\nu)}|\lambda|^{2/(2+\nu)}$ and therefore

$$f_V^2 \propto R_S^2(0)/\mu^3 \propto (L\mu)^{-3} \propto \mu^{-3(1+\nu)/(2+\nu)}|\lambda|^{3/(2+\nu)},$$

$$f_A^2 \propto R_P'^2(0)/\mu^5 \propto (L\mu)^{-5} \propto \mu^{-5(1+\nu)/(2+\nu)}|\lambda|^{5/(2+\nu)},$$

$$f_A^2/f_V^2 \propto (L\mu)^{-2} \propto \mu^{-2(1+\nu)/(2+\nu)}|\lambda|^{2/(2+\nu)}. \tag{11}$$

The logarithmic potential which describes ψ and Υ level spacing well leads to a drastic decrease: $f_A^2 \propto \mu^{-5/2}$ (and $f_V^2 \propto \mu^{-3/2}$). Even if we fix $\nu = -1/2$, such that $f_V^2 \propto \mu^{-1}$ (which is observed phenomenologically up to 10 GeV), f_A^2 decreases $\propto \mu^{-5/3}$.

There are some potentials, where the f's can be calculated explicitly. For a Coulombic potential $V = -\lambda/r$

$$f_V^2 = \frac{3}{16\pi}\lambda^3, \quad f_A^2 = \frac{3}{2^{10}\pi}\lambda^5,$$

$$f_A^2/f_V^2 = \lambda^2/64. \tag{12}$$

For a linear potential $V = Cr$

$$f_V^2 = \frac{3}{4\pi}\frac{C}{m^2}, \quad f_A^2 = \frac{9}{8\pi^{1/3}}\left(\frac{C}{m^2}\right)^{5/3},$$

$$f_A^2/f_V^2 = \tfrac{3}{2}\left(\frac{\pi C}{m^2}\right)^{2/3}, \tag{13}$$

where the WKB approximation has been used to calculate [I.3, III.2] f_A. For more realistic charmonium potentials R_S^2 and $R_P'^2$ have been determined numerically. $V(r) = -\lambda/r + a$ gives [IV.3] $R_S^2 = 0.81\ \text{GeV}^3$ and $R_P'^2 = 0.09\ \text{GeV}^5$ and thus ($m = 1.5$ GeV) $f_V^2 = 2.9 \times 10^{-2}$, $f_A^2 = 0.85 \times 10^{-2}$. QCD sum rules on the other hand [I.2] give $f_V^2 = 1.6 \times 10^{-2}$ and $f_A^2 = 0.93 \times 10^{-2}$.

From these results we can get some ideas about the order of magnitude[9] which one might expect for the presumed ($t\bar{t}$) and even heavier onia. The following four different model assumptions are used:

a) $\Gamma(1^{--})$ and f_A^2/f_V^2 remain mass independent. This is the most optimistic choice, but not very probable in potential models. The normalization is given by $f_A^2(M = M_{c\bar{c}}) = 0.93 \times 10^{-2}$.

---

[9] Rigorous results on the behaviour of $R_P'(0)$ in potential models can be found in Ref. [4].

b) All quantities scale as required for a logarithmic potential ($\nu = 0$).
c) Similar to b) but $\nu = -1/2$.
d) Coulomb like potential with $\lambda = 0.5$.

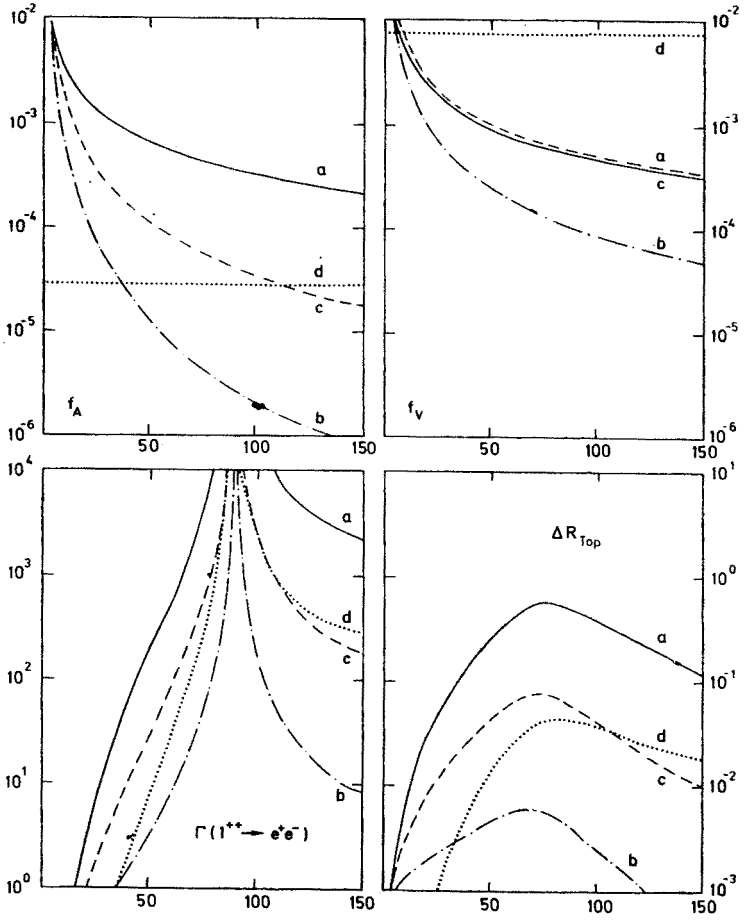

Fig. III.2

These models lead to the parametrizations

$$f_A^2 = \begin{cases} 0.93 \times 10^{-2} \left(\dfrac{3.5\ \text{GeV}}{M}\right)^{\beta}, & \beta = 1, \tfrac{5}{2}, \tfrac{5}{3} \text{ for a, b, c} \\ 2.9 \times 10^{-5} & \text{for d} \end{cases}$$

$$f_V^2 = \begin{cases} 1.6 \times 10^{-2} \left(\dfrac{3.1\ \text{GeV}}{M}\right)^{\beta}, & \beta = 1, \tfrac{3}{2}, 1 \text{ for a, b, c} \\ 7.5 \times 10^{-3} & \text{for d} \end{cases} \qquad (15)$$

which are displayed in Figs. III.2. a, b. In Figs. III.2. c, d I give the electronic width $\Gamma(1^{++} \to Z_0 \to e^+e^-)$, in eV, and the "enhancement" on top of the resonance

$$\Delta R_{\text{top}} \equiv \sigma_{\text{top}}/\sigma(e^+e^- \xrightarrow[\gamma,Z_0]{} \mu^+\mu^-), \tag{16}$$

using Eqs. (7) and (15) and an energy spread

$$\Delta E_{\text{CM}} = 20 \text{ MeV} \left(\frac{E_{\text{CM}}}{60 \text{ GeV}}\right)^2 \tag{17}$$

which corresponds to the dispersion in the LEP region[10].

Only under favorable circumstances (M = 50–100 GeV, favorable potential) may we expect ΔR around or above 0.05, which is certainly the minimal detectable value.

III.3. Electromagnetic backgrounds

Although this result is discouragingly small, I want to discuss briefly the experimental signal and in particular the electromagnetic background. Apart from measuring the total cross section one could hope to select the more specific decay channel of $^3P_1$ into $^3S_1$ and a photon which probably has a rather large branching ratio and thus enhances the signal/noise ratio.

In the following I shall therefore discuss two quite different electromagnetic processes (Fig. III.3):

a) The incoming e^+ or e^- radiates first a photon with $E = M_{1^{++}} - M_{1^{--}}$ resonance (Fig. III.3b). This is a nonresonating background for the reaction $e^+e^- \to 1^{++} \to 1^{--} + \gamma$ (Fig. III.3a).

b) Resonant formation of 1^{++} through two virtual photons (Fig. III.3c) which contributes to all channels.

Reaction a) has been calculated (Ref. [1]) and gives

$$\Delta R \approx \frac{9\Gamma(1^{--} \to e^+e^-)}{\alpha(M_{1^{++}} - M_{1^{--}})} \ln \frac{1+\Delta}{1-\Delta} \tag{18}$$

if the radiated photon is constrained within a region $\cos\theta \leqslant \Delta < 1$. For $\Delta = \cos 30°$, $\Gamma(1^{--} \to e^+e^-) = 5$ keV and $M_1^{++} - M_1^{--} = 400$ MeV the relative contribution is $\Delta R \approx 4\%$ which is quite comparable with the neutral current signal, but does not exhibit the resonance's rapid variation at $E_{\text{CM}} \approx M_1^{++}$.

Reaction b), the direct electromagnetic formation of 1^{++} contributes to all final states. It is not a serious background at high energies, but is interesting in its own right in particular for the charmonium system and applications to QCD. The evaluation is rather complicated and I shall just give the main results. The details can be found in Ref. [5]. At 3.5 GeV it dominates the neutral current completely, whereas the situation is reversed for heavier

[10] In general the energy spread is approximately given by $E_{\text{CM}} \approx 0.3 \times E_{\text{CM}}^2/\sqrt{\varrho}$ and ϱ, the bending radius, is 2344 m for LEP.

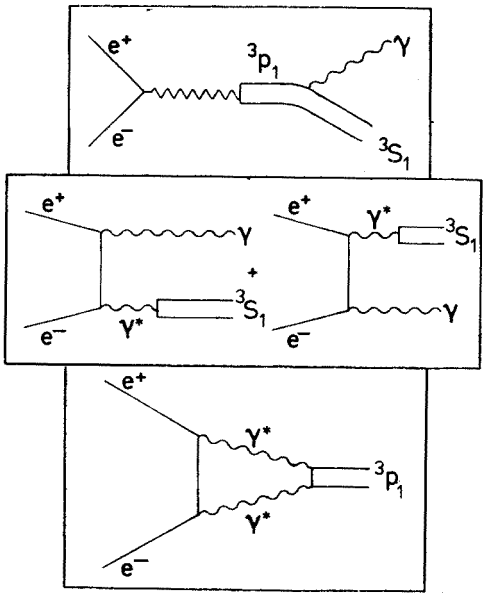

Fig. III.3

states ($M \geqslant M_\Upsilon$). Therefore I shall concentrate on the charmonium system and identify ^3P_J and $^3S_1$ with the χ_J and ψ particles.

To calculate the coupling of χ to two virtual photons, one has to resort to specific models. In the quarkonium model (Fig. III.4) χ is treated as a non-relativisitic bound-state and the amplitude is expanded in the relative velocity q/m_c. The $(\chi, \gamma^*, \gamma^*)$-coupling is then given by

$$A = i\sqrt{3}\,\hat{e}_c^2 e^2 32 \sqrt{\frac{3}{4\pi}}\, R'_P(0)\,[M^2 - p_1^2 - p_2^2 + bM - i\varepsilon]^{-2}$$

$$\times \{p_1^2\,\mathrm{Det}\,(\mathscr{E}, \mathscr{E}_1, \mathscr{E}_2, p_2) + (\mathscr{E}_1 p_1)\,\mathrm{Det}\,(\mathscr{E}, \mathscr{E}_2, p_1, p_2) + (1 \leftrightarrow 2)\}. \tag{19}$$

The final result is again proportional to the first derivative at the origin, however, it exhibits an additional logarithmic dependence on the binding energy

$$\Gamma(\chi_1 \to e^+e^-) = 3\hat{e}_c^4\alpha^4\,\frac{128}{\pi^2}\,\frac{|R'_P(0)|^2}{M^4}\left|\ln\frac{2b - i\varepsilon}{M}\right|^2. \tag{20}$$

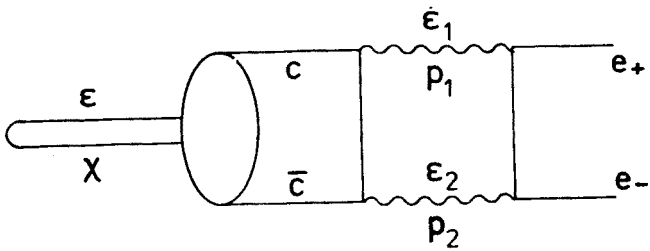

Fig. III.4

This logarithm shows up also in the result (Ref. [6]) for the reaction $\chi_1 \to \gamma e^+e^-$ and reflects the fact that the main contribution comes from the region, where one photon is soft and the other carries most of the momentum. Its magnitude is largely determined by the sign of the binding energy $b = 2m_Q - M$ and the numbers can be found in Tables III.I and III.II.

TABLE III.I

Ratio of electromagnetic to weak production, calculated through formulae (6), (20) with $b = \pm 0.5$ GeV

M(GeV)	3.5	10	35
e_Q	2/3	−1/3	2/3
EM/NC; $b = +0.5$ GeV	23	7.4×10^{-2}	2×10^{-2}
EM/NC; $b = -0.5$ GeV	170	21×10^{-2}	3.6×10^{-2}

For completeness I give in Table III.II also the results for the χ_2 particle. In the limit of $m_e \to 0$ the with for $\chi_0 \to e^+e^-$ is zero due to chiral invariance independent of any model. The ratio

$$\frac{\Gamma_{EM}}{\Gamma_{NC}} = \frac{2^9 \hat{e}_c^4 \alpha^4 \left| \ln \dfrac{2b - i\varepsilon}{M} \right|^2}{G_F^2 M^4} \tag{21}$$

decreases like M^{-4} and this is the reason why I concentrate entirely on charmonium.

TABLE III.II

$\Gamma(\chi_J \to e^+e^-)$ in eV under various assumptions

J	1	2
Quarkonium model (Eq.(8) $b = 0.5$ GeV)	0.023	0.013
Quarkonium model (Eq.(8) $b = -0.5$ GeV)	0.17	0.027
Vector dominance model (Eq.(21))	0.46	0.014
Generalized vector dominance model (Eq. (26))	0.08	0.005
Unitary limit (Eq. (22))	0.044	0.0023

Alternatively one can use vector dominance for the (χ, γ^*, γ^*)-coupling (Fig. III.5). Effectively this means to replace $(M^2 - p_1^2 - p_2^2 + bM - i\varepsilon)^{-2}$ by a formfactor[11] $\propto (p_1^2 - \mu^2)^{-1}(p_2^2 - \mu^2)^{-1}$. The ($\chi$, ψ, γ) and ($\psi\gamma$) couplings are adjusted to reproduce the widths $\Gamma(\chi \to \psi\gamma)$ and $\Gamma(\psi \to e^+e^-)$. Expanding in $(M-\mu)/M$ and keeping only the leading terms in the real and imaginary part gives

$$\Gamma(\chi_1 \to e^+e^-) = \tfrac{3}{2}\alpha M^2 \frac{\Gamma(\chi \to \psi\gamma)\Gamma(\psi \to e^+e^-)}{(4\pi)^2 (M-\mu)^3} \left| 1 - \pi\sqrt{3} - i4\pi \frac{M-\mu}{M} \right|^2. \tag{21}$$

[11] Here $\mu(\mu')$ denotes the mass of $\psi(\psi')$.

Note that the absorptive contribution is determined by the imaginary part alone and yields a model independent lower limit

$$\text{Abs}\,\Gamma = \tfrac{3}{2}\frac{\alpha}{E_\gamma}\Gamma(\chi \to \psi\gamma)\Gamma(\psi \to e^+e^-). \tag{22}$$

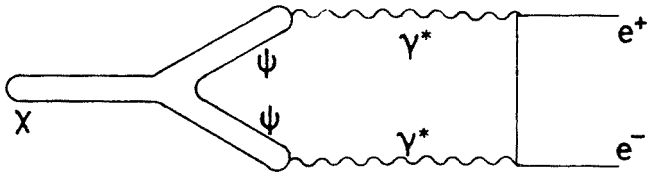

Fig. III.5

In Ref. [7] the effect of higher resonances like ψ' has been investigated more closely. They might enhance the effect or interfere destructively – depending on the sign of the various coupling constants. We start with an amplitude of the following form:

$$A(\chi\gamma^*\gamma^*) = e^2M^2\left[\frac{a^2f^2}{(p_1^2-\mu^2)(p_2^2-\mu^2)} + \frac{a'^2f'^2}{(p_1^2-\mu'^2)(p_2^2-\mu'^2)}\right.$$

$$\left. + \frac{aa'ff'}{(p_1^2-\mu^2)(p_2^2-\mu'^2)} + \frac{aa'ff'}{(p_1^2-\mu'^2)(p_2^2-\mu^2)}\right] \times \{\text{bracket from Eq. (19)}\}, \tag{23}$$

$f(f')$ is related to the electronic width of $\psi(\psi')$: $\Gamma = 4\pi/3\alpha^2\mu f^2$. From Eq. (11) we can deduce the amplitudes for $(\chi\psi\gamma)$ and $(\chi\psi'\gamma)$ coupling:

$$A(\chi\psi\gamma) = -eaM^2\left(\frac{af}{\mu^2} + \frac{a'f'}{\mu'^2}\right)\text{Det}\,(\mathscr{E}_\chi, \mathscr{E}_\psi, \mathscr{E}_\gamma, p_\gamma), \tag{24a}$$

$$A(\chi\psi'\gamma) = -ea'M^2\left(\frac{af}{\mu^2} + \frac{a'f'}{\mu'^2}\right)\text{Det}\,(\mathscr{E}_\chi, \mathscr{E}_{\psi'}, \mathscr{E}_\gamma, p_\gamma), \tag{24b}$$

and if we neglect the recoil on the ψ these reduce in fact to the well-known dipole transitions of nonrelativistic quantum mechanics. a and a' can now be calculated from

$$\Gamma(\chi \to \psi\gamma) = \alpha\left(\frac{af}{\mu^2} + \frac{a'f'}{\mu'^2}\right)^2 a^2\frac{(M^2-\mu^2)^3(M^2+\mu^2)}{24M\mu^2}, \tag{25a}$$

$$\Gamma(\chi \to \psi'\gamma) = \alpha\left(\frac{af}{\mu^2} + \frac{a'f'}{\mu'^2}\right)^2 a^2\frac{(\mu'^2-M^2)^3(M^2+\mu'^2)}{24M\mu'^2}. \tag{25b}$$

However, there is an ambiguity in the relative signs of a/f_V and a'/f_V' which has to be fixed theoretically. The relative sign of a and a' is in the potential model equal to the relative sign of the two dipole matrix elements, which equals the relative sign of $\int dr R_{1S}(r) r R_{1P}(r)$ and $\int dr R_{2S}(r) r R_{1P}(r)$. For a choice of wave functions such that $R(r) \xrightarrow[r\to\infty]{}$

+0 A. Martin has shown [8] that their sign is identical. With the same convention f_V and f_V' have opposite signs, because $R_{1S}(0) > 0$, while R_{2S} has a node and thus $R_{2S}(0) < 0$. Thus we deduce a relative minus between a/f_V and a'/f_V' and find for the generalized vector dominance model destructive interference between ψ and ψ' contribution.

$$\Gamma_{EM}(\chi_1 \to e^+e^-) = \frac{24\alpha}{(4\pi)^2}\Gamma(\chi \to \psi\gamma)\Gamma(\psi \to e^+e^-)\frac{\mu^5 M^2}{(M^2-\mu^2)^3(M^2+\mu^2)}$$

$$\times \left| F(\varrho)\frac{\left(1+\frac{a'}{a}\frac{f'}{f}\sqrt{\frac{R(\varrho')}{R(\varrho)}}\right)^2}{\left(1+\frac{a'}{a}\frac{f'}{f}\frac{\mu}{\mu'}\right)^2} - i\pi\frac{M^4-\mu^4}{\mu^2 M^2}\right|^2, \tag{26}$$

Here a'/a and f/f' can be deduced from the previous considerations, $\varrho = \mu^2/M^2$, $\varrho' = \mu'^2/M^2$, and $F(\varrho)$ is a complicated expression in terms of log, arctan and Spence functions [5]. Large cancelations between the ψ and ψ' amplitudes are found. While in Eq. (21) the contribution of the real part to Γ is roughly $14 \times \text{Abs}\,\Gamma$, in Eq. (26) the real part is only of the same magnitude as the imaginary part, which itself is of course the same in both models.

For a realistic treatment it would seem necessary to include also the higher resonances ψ'', ψ''', ... I do not want to pursue this because of various reasons: The (ψ'', χ, γ) couplings are unknown. The contributions above charm threshold are unknown and difficult to handle in the GVD model and finally we are in the moment (at the present state of experiment) interested rather in the qualitative aspects of the problem.

However, I want to emphasize that the destructive interference of ψ and ψ' contribution suggests that Eq. (21) gives rather an upper bound than a realistic value and therefore I estimate $\Gamma(\chi(3500) \to e^+e^-) = 0.1-0.5$ eV. The various model predictions are listed in Table II — together with the corresponding results for the $J = 2$ state.

Let me speculate whether the χ_1 could be produced directly at SPEAR or DORIS, using the most optimistic value $\Gamma(1^{++} \to e^+e^-) = 0.5$ eV.

The resonance enhancement of ψ is approximately a factor of 200 on top of the resonance. Thus, the ratio between the contribution from χ_1 on top of the resonance $\sigma_{top}(\chi_1)$ and the hadronic continuum σ_{cont} is given by $\sigma_{top}(\chi_1)/\sigma_{cont} = 200 \times \Gamma(\chi_1 \to e^+e^-)/\Gamma(\psi \to e^+e^-) = 0.02$ and the corresponding $R = \sigma_{top}(\chi_1)/\sigma_{\mu^+\mu^-} = 2.5 \times 0.02 = 0.05$. This small change of the total cross section is probably hard to detect — however, there are interesting channels, where the resonance enhancement is much stronger.

The branching ratio for $\chi \to \psi\gamma$ is roughly 35%. Thus, $\sigma_{top}(e^+e^- \to \chi_1 \to \psi\gamma)/\sigma_{\mu^+\mu^-} = 0.05 \times 0.35 = 0.0175$. The inevitable radiative tail of ψ contributes to R with 0.04, if we use only events where the angle between the γ and the beam is larger than 30°. Thus, on resonance there is a change in the fraction of hadronic events with one photon of energy $E_\gamma = E_{CM} - E_\psi$ from $0.04/2.5 = 0.016$ to $(0.04+0.0175)/2.5 = 0.023$. Can one detect such a change in the inclusive photon distribution? (with an integrated luminosity of 10^{36} cm^{-2} we would find 300 such photons off and 400 on resonance.)

A clear signal in an exclusive channel comes from the subsequent decay of the ψ into e^+e^- and $\mu^+\mu^-$ with a branching ratio of 7%+7%. This reduces the rate by a factor of 0.14. It corresponds to a fraction of hadronic event of $2.2^{\circ}/_{oo}$ off resonance and $3.2^{\circ}/_{oo}$ on resonance (with an integrated luminosity of 10^{36} cm^{-2} it corresponds to 45 such events off and 65 on resonance). e^+e^- machines with better energy resolution would of course enhance the resonance signal. The advantages of resonant χ_1 production would be:

a) Measurement of $\Gamma_{e^+e^-}$ and thus another test of charmonium dynamics.

b) More precise mass determination.

c) If the experiment could be done with a machine with better mass resolution, ($\Delta M \lesssim 0.5$ MeV) one could hope to measure the total width of χ_1.

Finally I want to mention that one can get predictions for hadronic χ production, which may be tested in the near future, if one translates the results from QED to QCD. These have been treated in Refs. [9, 10] and are beyond the scope of this lecture.

Let me summarize Chapter III: Direct formation of 1^{++} resonances through the neutral current tests the axial vector coupling of heavy quarks. The rates for heavy states depend sensitively on the choice of the potential, but are probably rather small ($R_{top} \lesssim 5\%$). Various electromagnetic background reactions have been calculaated. The $1^{++} \to (1^{--}+\gamma)$ final state gets a large contribution from the radiative tail of 1^{--}, which however does not resonate and gives just a smooth background.

The annihilation through two virtual photons is certainly negligible for masses above charmonium. For χ_1 (3500) however the electromagnetic amplitude dominates. To observe resonant production at 3.5 GeV would require e^+e^- machines with higher luminosity and (or) smaller energy spread ($\Delta M \lesssim 0.3$ MeV).

IV. SUPERHEAVY RESONANCES

IV.1. General remarks

Although the formulas were quite general, the results of the previous two chapters were concerned mainly with quarkonia of masses definitely below the mass of the Z_0, where neutral current effects could be considered as rather small compared to electromagnetic and strong interactions. There may however exist quarkonia with mass up to and even beyond the Z_0 mass and such states could eventually be detected at LEP. Weak and electromagnetic interactions are then equally important. Therefore I want to calculate electroweak couplings of such heavy states in a systematic manner.

LEP or any similar machine will probably run on the Z_0 resonance and one may ask for the decay rate of Z_0 into quarkonia together with a photon or the Higgs particle. Such decays would obviously test the coupling of heavy quarks to the Z_0 and to the photon or Higgs particle, and their rate has been calculated by Guberina, Kühn, Peccei and Rückl [III.2]. Unfortunately the branching ratios are tiny and thus will not be measured in the near future. The techniques for the evaluation of the amplitude and the results for the effective (Z_0, ($Q\bar{Q}$), H) and (Z_0, ($Q\bar{Q}$), γ) couplings may be useful also in a different context and therefore I will outline them in some detail in the second section.

In Section IV. 3a I will use these amplitudes and some results of Chapters II and III to evaluate all second order electroweak annihilations of all S- and P-wave states[12] (Figs. IV.1a-f).

a) $(Q\bar{Q}) \xrightarrow[\gamma, Z_0]{} f\bar{f}$

b) $(Q\bar{Q}) \xrightarrow[W \text{ exchange}]{} q\bar{q}$

c) $(Q\bar{Q}) \longrightarrow \gamma\gamma$

d) $(Q\bar{Q}) \longrightarrow H\gamma$

e) $(Q\bar{Q}) \longrightarrow Z\gamma$

f) $(Q\bar{Q}) \longrightarrow ZH$

and compare them with their lowest order QCD decay rate.

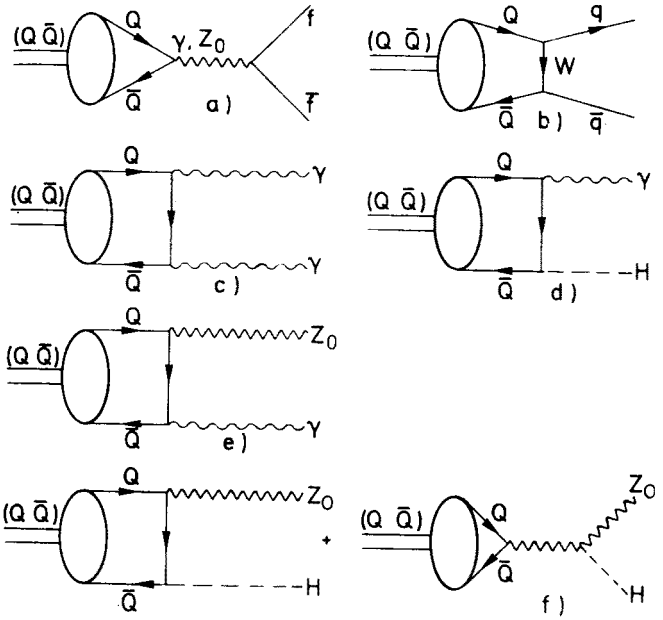

Fig. IV.1

The ratios of all these S-wave and P-wave decays are independent of assumptions about the potential model and thus test directly the Weinberg-Salam theory. The results for the decays e) and f) have not been published previously, the Higgs-photon decay of the $^1P_1$ state is new and the results for the W exchange contribution b) differs from previous ones in the literature.

[12] The decay into W^+W^- can be calculated in a straightforward fashion, using the same techniques. However, it is completely negligible compared to the single quark decay and shall be ignored.

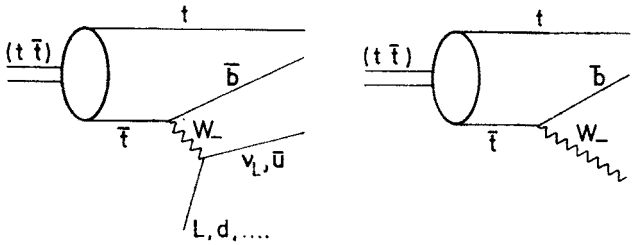

Fig. IV.2

In Section IV.3b I will contrast these processes with another decay mode, which becomes more and more relevant with increasing quark mass — the weak decay of a single quark.

For the toponium system this would be: $(t\bar{t}) \to t\bar{b}$ + leptons or hadrons (Fig. IV.2a). The t and b quarks may then either form a $(t\bar{b})$ meson or convert into a T and $\bar{B}$, eventually together with other light mesons. This decay mode has been suggested originally by Fujikawa [4] and specific calculations for the exclusive $(t\bar{b})$ channel have been performed by Bigi and Krasemann [5]. A measurement of these single quark decays would determine the presence or absence of large mixing angles, since one compares weak and electromagnetic or strong decays of the same particle and thus can determine the absolute magnitude of the coupling constants. In fact one finds that these decays will dominate for $M_Z \lesssim M_{Q\bar{Q}} < 2M_W$. For masses $M_Q > M_W$ single quark decays into W and a light quark (Fig. IV.2b) will take over.

IV.2. Quarkonia in Z_0 decays[13]

We now proceed to the calculation of Z_0 decays into onia and a photon or a Higgs meson and determine the amplitude for the couplings $(Z_0, (Q\bar{Q}), \gamma)$ and $(Z_0, (Q\bar{Q}), H)$. The amplitude for radiative decays of the Z_0 into an onium state is given, in general, by the sum of the first two diagrams of Fig. IV.3. For Higgs decay, because the Z_0 has a direct coupling to the Higgs meson, depending on the spin-parity of the onia, the third diagram of Fig. IV.3 may also enter. Let Q^μ be the total 4-momentum of the onia and q^μ be the relative 4-momentum between the quark and antiquark legs of Fig. IV.3, then the amplitude for radiative or Higgs decay can be written, schematically, as

$$A_{\chi,H} = \int \frac{d^4q}{(2\pi)^4} \operatorname{Tr} \mathcal{O}_{\gamma,H}(q)\chi(Q, q). \tag{1}$$

Here $\chi(Q, q)$ is the Bethe-Salpeter wavefunction appropriate to the given onium state, while $\mathcal{O}_{\gamma,H}(q)$ represents the rest of the matrix element depicted in Fig. IV.3. Specifically, for radiative decays we have[14].

---

[13] This part is based on work done in collaboration with B. Guberina, R. D. Peccei and R. Rückl. [III. 2]

[14] Our metric differs from the one used in Ref. [III. 2]: $g_{\mu\nu} = -\eta_{\mu\nu}$

$$\mathcal{O}_\gamma(q) = (g_V\gamma\mathscr{E}_Z + g_A\gamma\mathscr{E}_Z\gamma_5)\left[\frac{-(\gamma k+\gamma Q/2+\gamma q)-m}{(k+Q/2+q)^2-m^2}\right]e_q\gamma\mathscr{E}_\gamma$$

$$+e_q\gamma\mathscr{E}_\gamma\frac{(\gamma k+\gamma Q/2-\gamma q)-m}{(k+Q/2-q)^2-m^2}(g_V\gamma\mathscr{E}_Z+g_A\gamma\mathscr{E}_Z\gamma_5). \tag{2}$$

Here k^μ is the photon 4-momentum; $\mathscr{E}$ and $\mathscr{E}_Z$ are the polarization vectors of the photon and Z_0, respectively; e_q is the charge of the quark and g_V and g_A are the vector and axial coupling constants of the Z_0 to quarks as defined in Appendix A.

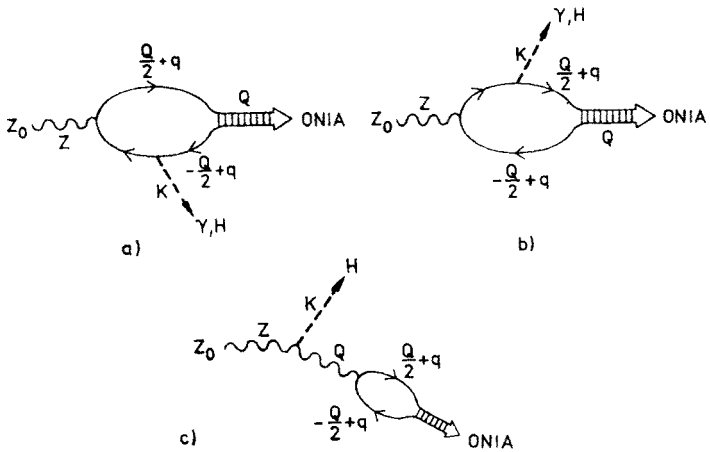

Fig.IV.3

For Higgs decays one has

$$\mathcal{O}_H(q) = (g_V\gamma\mathscr{E}_Z + g_A\gamma\mathscr{E}_Z\gamma_5)\left[\frac{-(\gamma k+\gamma Q/2+\gamma q)-m}{(k+Q/2+q)^2-m^2}\right]g_m$$

$$+g_m\left[\frac{(\gamma k+\gamma Q/2-\gamma q)-m}{(k+Q/2-q)^2-m^2}\right](g_V\gamma\mathscr{E}_Z+g_A\gamma\mathscr{E}_Z\gamma_5)+g_Z\left[\frac{\gamma\mathscr{E}_Z-\gamma Q\mathscr{E}_Z/M_Z^2}{M_Z^2-M^2}\right](g_V+g_A\gamma_5). \tag{3}$$

Here k^μ is now the Higgs momentum and the coupling constants g_m and g_Z are given by

$$g_m = m(\sqrt{2}\,G_F)^{1/2}, \tag{4a}$$

$$g_Z = 2M_Z^2(\sqrt{2}\,G_F)^{1/2}. \tag{4b}$$

To proceed, we shall adopt a nonrelativistic bound-state picture for describing the onia. The Bethe-Salpeter wavefunction $\chi(Q, q)$ can then be reduced to its nonrelativistic form. If we go to the rest system of the onia, and the system is nonrelativistic, the relative momentum between the quark and the antiquark pair is then much less than the mass

of the onia. That is, the bound-state wavefunction is sharply damped for relative momenta which become large on the scale of the onia's mass. This suggests that we may evaluate the decay amplitude in Eq. (1) by, essentially, neglecting the q-dependence of $\mathcal{O}(q)$. To be more precise, for S-wave onia we can replace $\mathcal{O}(q)$ by $\mathcal{O}(0)$ and thus the decay amplitude will be proportional to the value of the S-wave wavefunction at the origin. For P-waves, since the wavefunction vanishes at the origin, we must retain in $\mathcal{O}(q)$ terms linear in the relative momentum, obtaining then a result for the decay amplitude which is proportional to the derivative of the P-wave wavefunction at the origin. The above approximations of neglecting the q-dependence in $\mathcal{O}(q)$ are reasonable as long as the amplitude $\mathcal{O}(q)$ is itself not too strongly varying with q. For the problem at hand this is nearly always the case, unless the mass of the onia essentially coincides with that of the Z_0. We shall not worry about this singular case here, but shall comment upon it again later.

The evaluation of Eq. (1) can be done in a straightforward way and I have summarized the relevant formulas in Appendix B. After somewhat tedious algebraic manipulations one derives the relevant couplings for the various bound-states. The radiative decays are described by the following amplitudes:

$$A_\gamma(^1S_0) = -i\sqrt{\frac{48}{\pi M}}\left(\frac{e_q g_V R_S(0)}{M_Z^2 - M^2}\right)\varepsilon_{\mu\chi\tau\varrho}\varepsilon_Z^\mu \varepsilon_\gamma^\nu k^\tau Q^\varrho, \tag{5}$$

$$A_\gamma(^3S_1) = i\sqrt{\frac{48}{\pi M}}\left(\frac{e_q g_A R_S(0)}{M_Z^2 - M^2}\right) M\varepsilon_{\mu\nu\tau\varrho}\varepsilon_Z^\mu \varepsilon_\gamma^\nu k^\tau \varepsilon^\varrho, \tag{6}$$

$$A_\gamma(^1P_1) = i\sqrt{\frac{576}{\pi M}}\left(\frac{e_q g_A R_P'(0)}{M_Z^2 - M^2}\right)[(k\cdot\varepsilon_Z)(\varepsilon\cdot\varepsilon_\gamma) - (k\cdot\varepsilon)(\varepsilon_\gamma\cdot\varepsilon_Z)], \tag{7}$$

$$A_\gamma(^3P_0) = i\sqrt{\frac{48}{\pi M}}\left(\frac{e_q g_V R_P'(0)}{M_Z^2 - M^2}\right)\left(\frac{M_Z^2 - 3M^2}{M}\right)\left[\varepsilon_\gamma\cdot\varepsilon_Z - \frac{k\cdot\varepsilon_Z Q\cdot\varepsilon_\gamma}{k\cdot Q}\right], \tag{8}$$

$$A_\gamma(^3P_1) = \sqrt{\frac{1152}{\pi M}}\left(\frac{e_q g_V R_P'(0)}{M_Z^2 - M^2}\right)\left(\frac{M_Z^2}{M_Z^2 - M^2}\right)\varepsilon_{\mu\chi\tau\varrho}\varepsilon_Z^\mu \varepsilon_\gamma^\nu k^\tau \varepsilon^\varrho, \tag{9}$$

$$A_\gamma(^3P_2) = -i\sqrt{\frac{576}{\pi M}}\left(\frac{e_q g_V R_P'(0)}{M_Z^2 - M^2}\right) M\varepsilon_{\mu\nu}\left\{\varepsilon_Z^\mu \varepsilon_\gamma^\nu - \varepsilon_Z^\mu k^\nu \frac{Q\cdot\varepsilon_\gamma}{k\cdot Q}\right.$$

$$\left. + \frac{1}{k\cdot Q}[k^\mu k^\nu \varepsilon_\gamma\cdot\varepsilon_Z - k^\mu \varepsilon_\gamma^\nu k\cdot\varepsilon_Z]\right\}. \tag{10}$$

For Higgs decays, on the other hand, one finds

$$A_H(^1S_0) = -\sqrt{\frac{12}{\pi M}}(g_A(\sqrt{2}\,G_F)^{1/2}R_S(0))Q\cdot\varepsilon_Z, \tag{11}$$

$$A_H(^3S_1) = -\sqrt{\frac{12}{\pi M}}(g_V(\sqrt{2}\,G_F)^{1/2}R_S(0))$$

$$\times\left\{\frac{MM_Z^2}{M_Z^2-M^2}\mathscr{E}\cdot\mathscr{E}_Z+\frac{M(Q\cdot Z\mathscr{E}\cdot\mathscr{E}_Z-Q\cdot\mathscr{E}_Z Z\cdot\mathscr{E})}{M_Z^2+M_H^2-M^2}\right\}, \tag{12}$$

$$A_H(^1P_1) = \sqrt{\frac{144}{\pi M}}(g_V(\sqrt{2}\,G_F)^{1/2}R'_P(0))\frac{\varepsilon_{\mu\nu\tau\varrho}Z^\mu Q^\nu\mathscr{E}_Z^\tau\mathscr{E}^\varrho}{M_Z^2+M_H^2-M^2}, \tag{13}$$

$$A_H(^3P_0) = 0, \tag{14}$$

$$A_H(^3P_1) = -i\sqrt{\frac{288}{\pi M}}(g_A(\sqrt{2}\,G_F)^{1/2}R'_P(0))\left\{\frac{M_Z^2}{M_Z^2-M^2}\mathscr{E}\cdot\mathscr{E}_Z\right.$$

$$\left.+\frac{[M^2(M^2-M_H^2)\mathscr{E}\cdot\mathscr{E}_Z+Q\cdot Z(Z\cdot\mathscr{E}Q\cdot\mathscr{E}_Z-Q\cdot Z\mathscr{E}\cdot\mathscr{E}_Z)]}{(M_Z^2+M_H^2-M^2)^2}\right\}, \tag{15}$$

$$A_H(^3P_2) = \sqrt{\frac{576}{\pi M}}(g_A(\sqrt{2}\,G_F)^{1/2}R'_P(0))\frac{MZ_\alpha\mathscr{E}^{\alpha\beta}\varepsilon_{\mu\nu\varrho\beta}\mathscr{E}_Z^\mu Q^\nu Z^\varrho}{(M_Z^2+M_H^2-M^2)^2}. \tag{16}$$

Here $\mathscr{E}^\mu(\mathscr{E}^{\mu\nu})$ is the usual spin 1 polarization (spin 2 polarization tensor) vector, which obeys

$$Q^\mu\mathscr{E}_\mu = 0, \qquad \sum_{\mathscr{E}}\mathscr{E}_\mu\mathscr{E}_\nu = -g_{\mu\nu}+\frac{Q_\mu Q_\nu}{M^2}\equiv P_{\mu\nu}, \tag{17}$$

$$\mathscr{E}^{\mu\nu} = \mathscr{E}^{\nu\mu}, \qquad \mathscr{E}^\mu_\mu = 0, \qquad Q^\mu\mathscr{E}_{\mu\nu} = 0,$$

$$\sum_{\mathscr{E}}\mathscr{E}_{\mu\nu}\mathscr{E}_{\alpha\beta} = \tfrac{1}{2}[P_{\mu\alpha}P_{\nu\beta}+P_{\nu\alpha}P_{\mu\beta}]-\tfrac{1}{3}P_{\mu\nu}P_{\alpha\beta}, \tag{18}$$

Q, Z and k are the boundstate, Z_0 and Higgs or photon momenta. $R_S(0)$ and $R'_P(0)$ refer to the radial wavefunction of the S and P state. The amplitudes are still completely general. In Section IV.3a they will be related to the amplitudes for decays of onia into Z_0 and photons or Higgs, and substituting g_V by e_q we can also find the decays into a photon and a Higgs particle.

First I will use them to derive the Z_0 decays. The evaluation is straightforward. To gauge the magnitude of our results it is useful to compare them with the $Z_0 \to \mu^+\mu^-$ rate, which has a branching fraction of roughly 3%. Obviously one also has to make some assumptions about the magnitude of the wave functions R_S and R_P and their mass dependence. Various scaling laws and their relation to potentials have been discussed in Section III.2. In Fig. IV.4, taken from Ref. [III.2], I give the ratios

$$R_{\gamma,H}(^{2S+1}L_J) = \frac{\Gamma(Z_0 \to {}^{2S+1}L_J+\gamma, H)}{\Gamma(Z_0 \to \mu^+\mu^-)} \tag{19}$$

for $e_q = 2/3$ and $\sin^2\theta_W = 0.23$. As wavefunctions we used

$$R_S^2(0) = 0.05\ \text{GeV} \times M^2,$$

$$R_P'^2(0) = 1.25 \times 10^{-4}\ \text{GeV} \times M^4, \tag{20}$$

which corresponds to

$$f_V^2 = 1.54 \times 10^{-2}\left(\frac{3.1\ \text{GeV}}{M}\right),$$

$$f_A^2 = 0.82 \times 10^{-3}\left(\frac{3.5\ \text{GeV}}{M}\right). \tag{21}$$

For any other assumption about the wave functions our results can easily be translated.

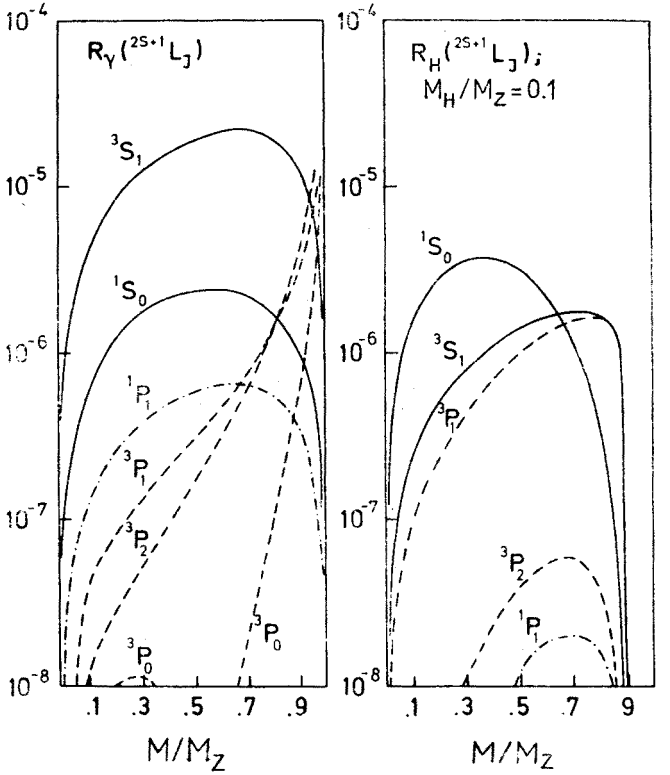

Fig. IV.4

Let me conclude with the following comments on Fig. IV.4:

a) All rates are extremely small with the best decays, $Z_0 \to \gamma + {}^3S_1$, and $Z_0 \to$ Higgs $+ {}^3S_0$, being of the order of $10^{-5} - 10^{-6}$ the $Z_0 \to \mu^+\mu^-$ rate.

b) The Higgs rates have been calculated for $M_H/M_Z = .1$. Increasing the mass of the Higgs in general has a tendency to depress these rates further.

c) The peaking of the decay rates for $Z_0 \to \gamma + {}^3P_J$ for $(M/M_Z) \to 1$ is probably not to be trusted past, say, $(M/M_Z)^2 \approx .9 - .95$. This peaking is a result of the vanishing of the denominator in the propagator term in $A_\gamma({}^3P_J)$. However, as we have commented upon earlier, when this happens the approximation of neglecting the relative momentum dependence in calculating the decay amplitude is not reliable.

d) To detect specifically the Higgs meson this way would require identifying the onium, e.g., the ${}^3S_1$ final state through its leptonic decay mode, which in general leads to an extremely small overall branching ratio. The sharp photon line, which would be in principle a signal for the radiative decay $Z_0 \to \gamma + (Q\overline{Q})$ will be buried in the continuum background coming from ordinary bremsstrahlung, e.g., from $Z_0 \to \mu^+\mu^-\gamma$.

e) Our assumptions about the mass dependence of R_S and R'_P were not very elaborate. Still any reasonable assumption does not increase the results by orders of magnitude. If the toponium is found, more reliable calculations will be possible, using the observed level spacings.

The preceding discussion has made it quite clear that it will be essentially impossible to detect the Z_0 decays under discussion. Quarkonium $+\gamma$ populates such a small portion of the $Q\overline{Q}\gamma$ phase space that its formation is highly suppressed compared to the two jet plus photon production. Still the amplitudes, as derived in Eqs. (5)–(16), will be useful to estimate all kinds of electroweak decays of superheavy onia.

IV.3a. Electroweak annihilation of onia

It has been stated frequently that weak decays are as important as electromagnetic and strong decays for extremely massive onia [1–6]. I shall now give a systematic treatment of second order decays of S- and P-wave onia, as listed in Section IV.1. All those, which are calculated in this section require the annihilation of both Q and $\overline{Q}$ ("annihilation decays") and thus are proportional to the wavefunction at the origin $R_S(0)$ or the first derivative $R'_P(0)$. Since the main interest is in the corresponding branching ratios, I will give the ratios

$$R(S) \equiv \Gamma/\Gamma_S \quad \text{and} \quad R(P) \equiv \Gamma/\Gamma_P \tag{22}$$

for S and P waves, respectively. Γ_S stands for the electronic decay rate of ${}^3S_1$ through a virtual photon

$$\Gamma_S \equiv 4\alpha^2 \hat{e}_Q^2 R_S^2(0) M^{-2} \tag{23}$$

and Γ_P is the two photon decay rate of ${}^3P_0$.

$$\Gamma_P \equiv \Gamma({}^3P_0 \to \gamma\gamma) = 432\alpha^2 \hat{e}_Q^4 R'^2_P(0) M^{-4}. \tag{24}$$

The leptonic and hadronic decays of $^3S_1$ through the photon and Z_0 (Fig. IV.1a) are only possible for vector and axial states. The results for $^3S_1$ have often been quoted

$$R(^3S_1 \to f\bar{f}) = C_f\left(\hat{e}_f^2 + \frac{v_Q^2(v_f^2+a_f^2)}{\hat{e}_Q^2}\,\frac{\mu^4}{(\mu^2-1)^2+\mu_\Gamma^2} + 2\,\frac{v_Q v_f}{\hat{e}_Q}\,\frac{\mu^2(\mu^2-1)}{(\mu^2-1)^2+\mu_\Gamma^2}\right). \tag{25}$$

Here $\mu \equiv M/M_Z$, $\mu_\Gamma \equiv \Gamma(Z \to \text{all})/M_Z$, $C_f = 1$ for leptons and 3 for quarks. The ratios of neutral current and electromagnetic couplings v and a are defined in Appendix A.

The corresponding reaction for $^3P_1$ proceeds through the neutral current only and has been discussed in Chapter III.

$$R(^3P_1 \to f\bar{f}) = \tfrac{2}{3}\,C_f\,\frac{a_Q^2(v_f^2+a_f^2)}{\hat{e}_Q^4}\,\frac{\mu^4}{(1-\mu^2)^2+\mu_\Gamma^2}. \tag{26}$$

A closely related process is the decay of Q and $\bar{Q}$ through W exchange (Fig. IV.1b) into their weak isospin partner, e.g., $(t\bar{t}) \to b\bar{b}$. The amplitude can be obtained from the previous considerations in a straightforward manner. As long as the momentum transfer in the t channel is small[15] compared to M_W, one uses the Fierz transformed amplitude and applies again the methods leading to Eqs. (III.9,10) for f_V^2 and f_A^2. From the V-A structure of the original and the transformed amplitude it is obvious that the W exchange contributes only to $^3S_1$ and $^3P_1$ decays, just like before. The relative weight of annihilation through W exchange and through Z_0, depends of course also on mixing angles, which I have ignored for the moment. In fact this reaction offers the interesting possibility to measure this angle — just like in the single quark decay, which will be discussed in Section IV.3b. It is furthermore important to realize that one has to add the *amplitudes* which come from annihilation through γ and Z_0 and from W exchange[16]. For the total amplitude for the decay $(t\bar{t}) \to b\bar{b}$ one finds

$$A(^3S_1 \to b\bar{b}) = \sqrt{3}\,f_V\mu^2e^2\left\{\left[\frac{\hat{e}_t\hat{e}_b}{\mu^2} + \frac{v_t v_b}{(\mu^2-1)+i\mu_\Gamma} - \tfrac{2}{3}\,\frac{a^2}{(1+\mu^2/4\cos^2\theta_W)}\right]\bar{b}\gamma\mathcal{E}b\right.$$
$$\left. + \left[\frac{v_t a_b}{(\mu^2-1)+i\mu_\Gamma} + \tfrac{2}{3}\,\frac{a^2}{(1+\mu^2/4\cos^2\theta_W)}\right]\bar{b}\gamma\mathcal{E}\gamma_5 b\right\}, \tag{27a}$$

$$A(^3P_1 \to b\bar{b}) = \sqrt{3}\,f_A\mu^2e^2\left\{\left[\frac{a_t v_b}{(\mu^2-1)+i\mu_\Gamma} + \tfrac{2}{3}\,\frac{a^2}{(1+\mu^2/4\cos^2\theta_W)}\right]\bar{b}\gamma\mathcal{E}b\right.$$
$$\left. + \left[\frac{a_t a_b}{(\mu^2-1)+i\mu_\Gamma} - \tfrac{2}{3}\,\frac{a^2}{(1+\mu^2/4\cos^2\theta_W)}\right]\bar{b}\gamma\mathcal{E}\gamma_5 b\right\}. \tag{27b}$$

The relative decay rates are shown in Fig. IV.5 together with the corresponding curves for leptonic and other quark decays, and for comparison also the hadronic rates

---

[15] Cf. the discussion in Chapter V. 1.

[16] This has been overlooked by the authors of Ref. [3–5] who considered the W exchange separately.

are given (Eqs. (44–49)). $u\bar{u}$ and ss are even slightly suppressed at medium energies due to destructive interference of electromagnetic and neutral current; there is, however, a dominating constructive contribution from the W exchange for decays into $b\bar{b}$. For $M \to M_Z$ the Z_0 pole gives of course the overwhelming contribution.

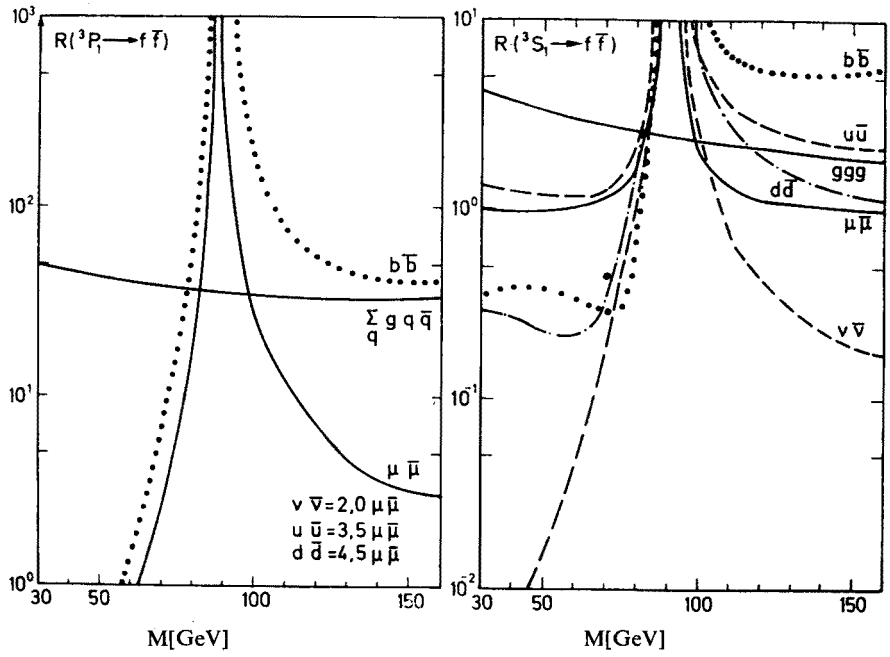

Fig. IV.5

Experimentally, all these fermionic decays should manifest themselves through their two jet structure, and specifically the decays into $b\bar{b}$ could be identified through the characteristic signature of b decays. The decay into neutrinos on the other hand may have a branching ratio up to 10% ($M \gtrsim 70$ GeV) and under such favorable circumstances it might be tagged in the cascade decay $2\,^3S_1 \to 1\,^3S_1 + \pi\pi\text{—}\nu\bar{\nu} + \pi\pi$ [7]. For quarkonium masses close to the Z pole the decays of 1^{--} and 1^{++} states are dominated by the fermionic decays through the virtual Z_0. An alternative way to describe this situation is through mixing of vector and axial states with the Z_0 [8].

For completeness and comparison I list the well-known two photon decays of the $C = +1$ quarkonia

$$R(^1S_0) = 3\hat{e}_Q^2, \quad R(^3P_0) \equiv 1, \quad R(^3P_2) = 4/15. \tag{28}$$

The decay of a heavy $^3S_1$ onium into the Higgs meson and a photon has been proposed as a promising source of Higgs particles [9]. This mode can be identified either through the monoenergetic photon or through the characteristic decays of the H. This transition should be more and more important for heavier onia, since the Higgs coupling is proportion-

al to the quark mass. It is only possible for $C = -1$ states. The $^3S_1$ decay has been calculated previously [9]

$$R(^3S_1 \to H\gamma) = \frac{G_F}{\sqrt{2}\,4\pi\alpha}(M^2 - M_H^2) \tag{29}$$

and the result for $^1P_1$ can be obtained, using a modified version of Eq. (13)

$$R(^1P_1 \to H\gamma) = \frac{1}{9\hat{e}_Q^2}\,\frac{G_F}{\sqrt{2}\,4\pi\alpha}(M^2 - M_H^2). \tag{30}$$

In Fig. IV.6 the relative rate is given for the $^3S_1$ assuming $M_H = 10$ GeV.

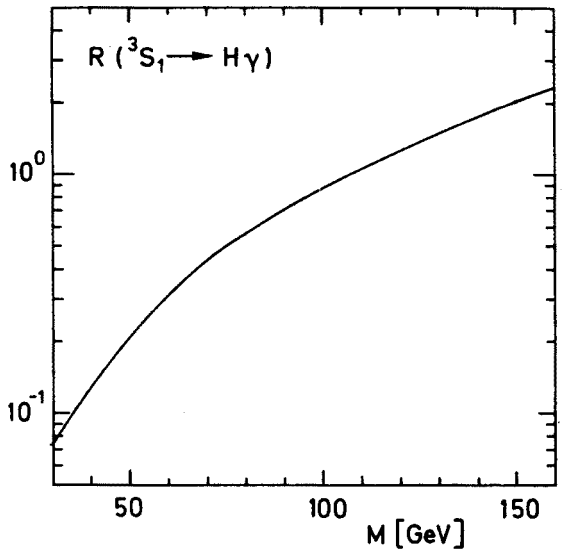

Fig. IV.6

All the previously discussed decays are already relevant for masses below M_Z. Beyond this other electroweak decays come into play which are as important as the fermionic decays, namely, decays into Z_0 and a photon or a Higgs particle. Thus the structure of quarkonium annihilation decays becomes increasingly complex once we are beyond the Z_0 pole. In fact it may well be that none of the individual channels will ever be resolved — in particular since single quark decays will finally take over.

The Z_0 couples to quarks with vector and axial coupling and thus the $(Z\gamma)$- and (ZH)-decay modes are possible for nearly all the various spin parity states. The rates can be calculated with the help of the amplitudes for Z_0 decays (Eq. (5–16)), which, after crossing, apply also to the decays under consideration. The complete list of all the corresponding ratios reads as follows:

$$R_{\gamma Z}(^1S_0) = 6\,\frac{v_Q^2}{\mu^2}(\mu^2 - 1), \tag{31}$$

$$R_{\gamma Z}({}^3S_1) = 2a_Q^2/\mu^2(\mu^4-1), \tag{32}$$

$$R_{\gamma Z}({}^1P_1) = 2/(9\hat{e}_Q^2)a_Q^2/\mu^2(\mu^4-1), \tag{33}$$

$$R_{\gamma Z}({}^3P_0) = 2/(9e_Q^2)v_Q^2/\mu^2(\mu^2-1)^{-1}\,(1-3\mu^2)^2, \tag{34}$$

$$R_{\gamma Z}({}^3P_1) = 4/(9\hat{e}_Q^2)v_Q^2/\mu^2(\mu^2-1)^{-1}\,(1+\mu^2), \tag{35}$$

$$R_{\gamma Z}({}^3P_2) = 4/(45\hat{e}_Q^2)v_Q^2/\mu^2(\mu^2-1)^{-1}\,(1+3\mu^2+6\mu^4), \tag{36}$$

$$R_{HZ}({}^1S_0) = 3/(2\hat{e}_Q^2)a_Q^2/\mu^2\varrho^3, \tag{37}$$

$$R_{HZ}({}^3S_1) = 1/(2\hat{e}_Q^2)v_Q^2/\mu^2(1+\mu_H^2-\mu^2)^{-2}$$

$$\times\left\{\left[1-\mu^2+\mu_H^2\,\frac{2\mu^2-\mu_H^2}{1-\mu^2}\right]^2+2\mu^2\left[1-\mu^2+\mu_H^2\,\frac{3-\mu^2}{1-\mu^2}\right]^2\right\}, \tag{38}$$

$$R_{HZ}({}^1P_1) = 1/(9\hat{e}_Q^4)v_Q^2\varrho^3(1+\mu_H^2-\mu^2)^{-2}, \tag{39}$$

$$R_{HZ}({}^3P_0) = 0, \tag{40}$$

$$R_{HZ}({}^3P_1) = 1/(18\hat{e}_Q^4)a_Q^2/\mu^2\varrho(1+\mu_H^2-\mu^2)^{-4}$$

$$\times\{2(1+\mu^2-\mu_H^2)^2\,[(1-\mu^2)^2+\mu_H^2(2-\mu^2+\mu_H^2(1-\mu^2)^{-1}]^2$$

$$+\mu^2[3(1-\mu^2)^2+\mu_H^2(10-2\mu^2+\mu_H^2(3+\mu^2)\,(1-\mu^2)^{-1})]^2\}, \tag{41}$$

$$R_{HZ}({}^3P_2) = 1/(30\hat{e}_Q^4)\varrho^5(1+\mu_H^2-\mu^2)^{-4}. \tag{42}$$

Here I have defined scaled masses

$$\mu^2 = M^2/M_Z^2, \quad \mu_H^2 = M_H^2/M_Z^2,$$

$$\varrho^2 = 1+\mu^4+\mu_H^4-2\mu^2-2\mu_H^2-2\mu^2\mu_H^2 \tag{43}$$

and v and a are defined in Appendix A.

The ratios are plotted in Figs. IV.7a-f as a function of M and a Higgs mass of 10 GeV was assumed for definiteness. For comparison also the hadronic rates, as calculated in QCD, are shown here:

$$R_{gg}({}^1S_0) = \tfrac{2}{3}\,\frac{\alpha_s^2}{\alpha^2\hat{e}_Q^2}, \tag{44}$$

$$R_{ggg}({}^3S_1) = \tfrac{10}{81}\,\frac{\pi^2-9}{\pi}\,\frac{\alpha_s^3}{\alpha^2\hat{e}_Q^2}, \tag{45}$$

$$R_{ggg}({}^1P_1) = \frac{20}{3^5\pi}\,\frac{\alpha_s^3}{\alpha^2\hat{e}_Q^4}\,\ln\frac{M}{\Delta}, \tag{46}$$

$$R_{gg}(^3P_0) = \tfrac{2}{9}\frac{\alpha_s^2}{\alpha^2\hat{e}_Q^4}\,, \tag{47}$$

$$R_{gq\bar{q}}(^3P_1) = N_q\frac{8}{3^5\pi}\frac{\alpha_s^3}{\alpha^2\hat{e}_Q^4}\ln\frac{M}{\Lambda}\,, \tag{48}$$

$$R_{gg}(^3P_2) = \tfrac{8}{135}\frac{\alpha_s^2}{\alpha^2\hat{e}_Q^4}\,. \tag{49}$$

For the curves $\Lambda = 1$ GeV was chosen as infrared cutoff, $\alpha_s = 1\Big/\left(4+\frac{25}{12\pi}\log M^2\Big/10\right)$ as strong coupling constant and $N_q = 5$. The solid (dashed, dotted) lines refer to the strong (γZ, HZ) decay.

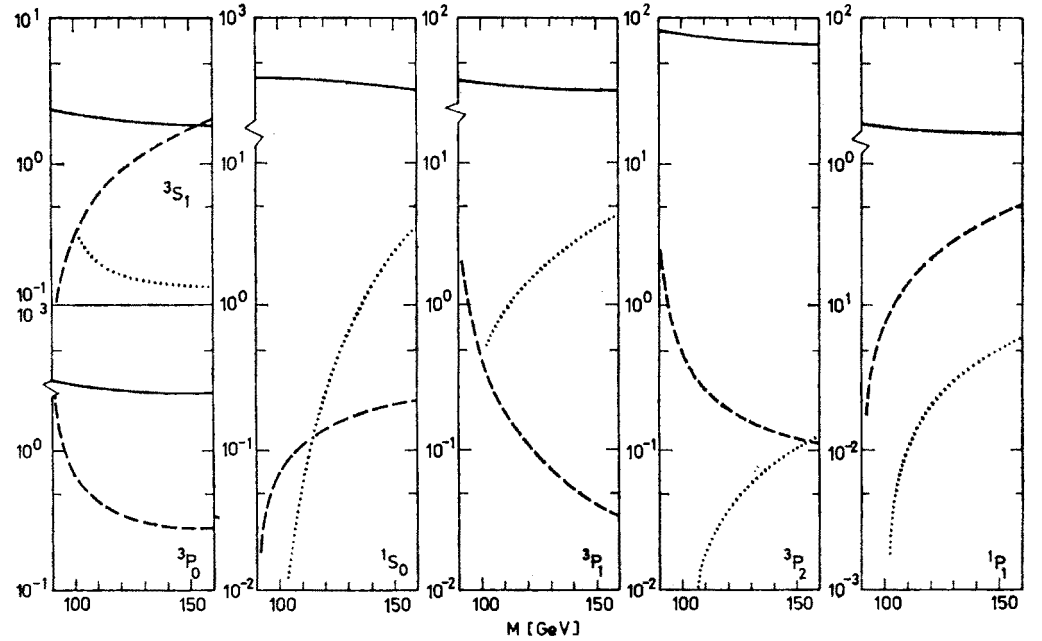

Fig. IV.7

Let me conclude this part with several comments:

a) The results, which are displayed in Figs. IV.5–7, show that all electroweak annihilation decays are of comparable strength for superheavy onia and they compete well with ordinary hadronic decays. Any individual decay channel however will be rather hard to identify because of the large number of decay modes.

b) In the intermediate region — roughly up to 80 GeV — the importance of fermionic decays increases gradually mainly because of the decrease of strong decays and the increasing importance of the neutral current for 1^{--} and 1^{++} states. Between 80 GeV and 100 GeV their decays are completely dominated by the Z_0. Beyond 100 GeV ($Z_0\gamma$) and (Z_0H) decays are as important as the other annihilation channels. However, as we shall see in

Section IV.3b, in the same region the single quark decay takes over and changes the pattern of quarkonium decays completely.

c) In some decay rates one finds denominators like $(\mu^2-1)^{-1}$, which are quite singular for $\mu^2 \to 1$. It is in this region, where the short distance approximation, as discussed in Appendix B, breaks down. The virtual heavy quark is no longer far off shell; it may have time for soft interactions with its quark partner and exchange many soft gluons (Fig. IV.8a). A more reasonable treatment would then proceed through a vector dominance model (Fig. IV.8b).

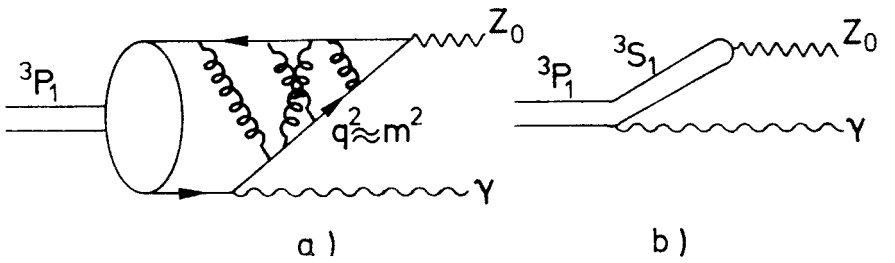

Fig. IV.8

d) The decays $(Q\bar{Q}) \to W^+W^-$ and $(Q\bar{Q}) \to HH$ are the only remaining second order electroweak decays. They can be evaluated in a straightforward manner with the methods of Appendix B. The first one is possible only beyond 150 GeV, at masses where the single quark decay dominates already completely and thus it will never be detected. The second one is experimentally rather hard to identify, since it is possible only for $^3P_0$ and $^3P_2$. Therefore I will not bother to evaluate these transitions here.

e) The formulas, derived in Sections IV.3a and IV3b are quite useful also for the calculation of other transitions, which involve quarkonia. For example, it has been speculated that the Higgs meson and the $^3P_0$ state of $(b\bar{b})$ could be nearly degenerate [10]. Then the relevant parameter is the amplitude for the coupling of $^3P_0$ and H, which is

$$|A(^3P_0 \to H)| = \frac{27}{\pi} R'_P(0) M(\sqrt{2}\, G_F) \tag{50}$$

and can be calculated from Eqs. (4a) and (B.14). Similarly to Eqs. (29, 30) one can evaluate the inverse reaction, namely, Higgs decays into onia and a photon. The result for the $^3S_1$ state has been given previously [11]

$$\frac{\Gamma(H \to {}^3S_1 + \gamma)}{\Gamma(^3S_1 \underset{\gamma}{\to} e^+e^-)} = \frac{3G_F}{4\sqrt{2}\,\pi\alpha}\left(\frac{M}{M_H}\right)^3 (M_H^2 - M^2) \tag{51}$$

and the rate for the $^1P_1$ state is

$$\frac{\Gamma(H \to {}^1P_1 + \gamma)}{\Gamma(^3P_0 \to \gamma\gamma)} = \frac{3G_F}{4\sqrt{2}\,\pi\alpha}\,\frac{1}{9\hat{e}_Q^2}\left(\frac{M}{M_H}\right)^3 (M_H^2 - M^2). \tag{52}$$

The prospects for measuring these reactions are not very promising.

IV.3b. Single quark decays

Now I turn to the decay mode, which will be of increasing importance for heavy onia — the single quark decay [1–6]. All the previous decay modes were proportional to the probability that the two constituents annihilate and thus proportional to the wavefunction at the origin. There is however the chance that one quark decays into its (weak) isospin partner and the other quark survives and can be treated as spectator (Fig. IV.2). This mode is not inhibited by any wavefunction effects and will therefore dominate for extremely large masses. The rate for toponium decay is given by

$$\Gamma_{SQ} = 2\times 9\times \frac{G_F^2 m_Q^5}{192\pi^3} f\left(\frac{m_Q^2}{M_W^2}, \frac{m_q^2}{m_Q^2}\right), \tag{53}$$

$$f(\varrho,\mu) = 2\int_0^{(1-\sqrt{\mu})^2} du \left(\frac{1}{1-u\varrho}\right)^2 [(1-\mu)^2+u(1+\mu)-2u^2]\Delta(1,\mu^2,u^2)$$

$$= \begin{cases}(1-\mu)(1-8\mu+\mu^2)-12\mu^2\ln\mu & \text{for } \varrho = 0\\ 2\varrho^{-4}[6(\varrho+(1-\varrho)\ln(1-\varrho))-3\varrho^2-\varrho^3] & \text{for } \mu = 0'\end{cases}$$

where the effect of the W-propagator and of the b mass ($= m_q$) has been taken into account. The function f is displayed in Fig. IV.9.

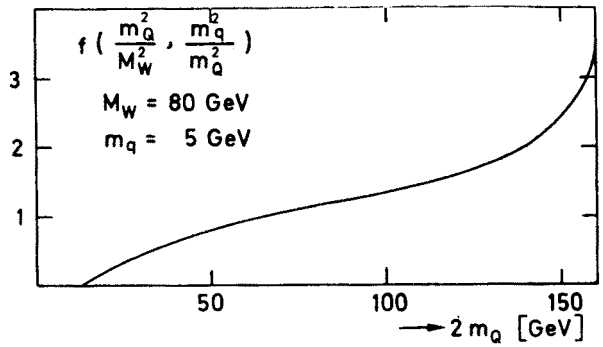

Fig. IV.9

In Fig. IV.10 this rate is compared with the total fermionic rate $\sum_f \Gamma(^3S_1 \to f\bar{f})$, assuming Γ_S independent of M. Already for $M \gtrsim 50$ GeV one gets a quite significant contribution, which amounts to more than 5% branching ratio and for $M \gtrsim 120$ GeV this mode dominates completely. For $M > 2(M_W+m_q)$ the decay into a real W and the isodoublet partner takes rapidly over:

$$\Gamma_W = 2\frac{G_F}{8\pi\sqrt{2}} m_Q^3 \left(1+2\frac{M_W^2}{m_Q^2}\right)\left(1-\frac{M_W^2}{m_Q^2}\right)^2. \tag{54}$$

All these decays can in principle be inhibited by mixing angles. Since they compete with and can be compared to electromagnetic and strong decays, they offer the unique possibility to gauge the magnitude of weak decays of heavy quarks. This holds in particular if a seventh quark and the corresponding onium should ever be found. Lifetime measurements which are the other alternative — used successfully for D-decays — will probably not be feasible for the corresponding heavy mesons or baryons.

Is there a simple way to identify and isolate single quark decays among the many different and complicated final states? It has been proposed [3, 5] that they could be a source of $(t\bar{b})$ mesons (Fig. IV.2a), which might give a clear signal in specific channels. In a specific model calculation using harmonic oscillator wavefunctions, Bigi and Krasemann [5] find that only a rather small fraction (18%–3% for $M = 35-80$ GeV) of t and $\bar{b}$ combines into a $(t\bar{b})$ meson and their decays are again difficult to identify. The decay

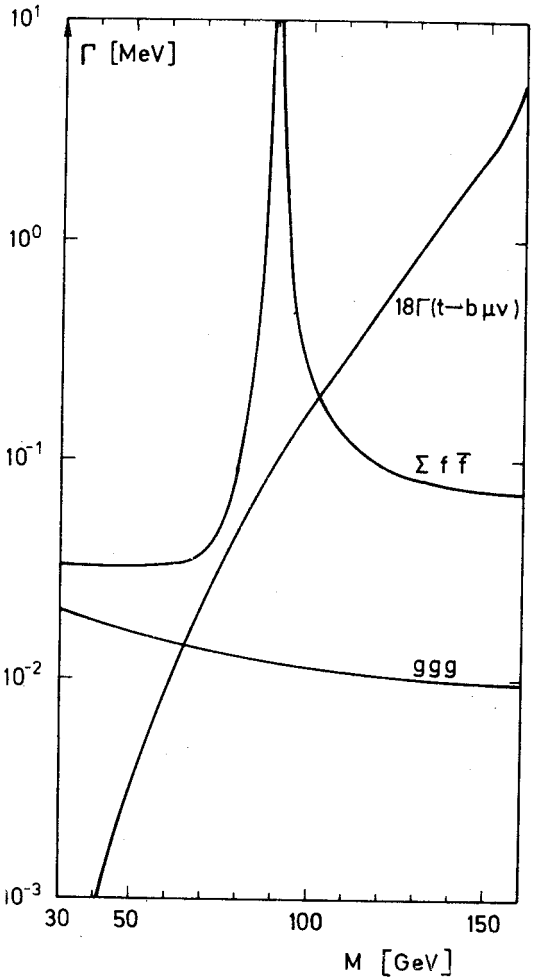

Fig. IV.10

into T and B (Fig. IV.2b) should manifest itself in a rather large leptonic and kaon yield. Particularly, multilepton events might lead to rather striking signals for this interesting decay mode. In principle it could be confused with the fermionic decays into $b\bar{b}$, which lead to a similar signature. If one compares their rates, then one finds that the single quark decay dominates in most mass regions.

To summarize: single quark decays get rapidly important for quarkonium masses beyond 40 GeV. Multi-lepton and multi-kaon events are clear signatures for such decays. They gauge the magnitude of mixing angles.

V. PARITY MIXING OF ONIA

V.1. General remarks

It has been predicted [1] a long time ago that one observable effect of neutral currents should be the mixing of atomic levels with different parities. Such a parity violation has been observed experimentally some time ago [2] despite the smallness of the relevant energies and mixing angles. For heavy quarkonia the typical masses and momenta are far larger than for atoms and one might therefore expect relatively larger effects.

Quarkonia are eigenstates of parity *and* charge conjugation, which however may mix through the neutral current. It is in fact the violation of C which could help to detect the mixing: the $2\,^3S_1$ state ($J^{PC} = 1^{--}$) mixes with the $1\,^3P_1$ state ($J^{PC} = 1^{++}$) and through this the direct decay $(2\,^3S_1) \to \gamma + (1\,^3S_1)$ is allowed.

In the following I shall present unpublished results on this subject. In Section V.2 I show that the only possibility for parity mixing of quarkonia is that of 1^{++} and 1^{--} levels and evaluate the magnitude of the mixing angles. In Section V.3 the rate of the radiative transition $(2\,^3S_1) \to \gamma + (1\,^3S_1)$ is calculated, including all possible mixing effects. Section V.4 finally contains some numerical examples, based on specific potential models, and the conclusions.

V.2. The mixing angles

In the standard quarkonium spectroscopy the levels are eigenstates of J^{PC}. The P and C violating neutral current will lead to transitions between levels of different P and C; the total angular momentum J however has to remain unchanged. Thus one might expect mixing of the lowest lying states $^1S_0$ (0^{-+}) and $^3P_0$ (0^{++}) or of $^3S_1$ (1^{--}), $^3P_1$ (1^{++}) and $^1P_1$ (1^{-+}). Since we are furthermore interested only in CP conserving interactions, the only remaining possibility is the mixing between vector and axial states, and I shall concentrate on the lowest levels $1\,^3S_1$, $2\,^3S_1$ and $1\,^3P_1$.

The mixing angles are defined through

$$|\tilde{1}\rangle = |1\rangle + \theta_1 |P\rangle,$$

$$|\tilde{2}\rangle = |2\rangle + \theta_2 |P\rangle, \tag{1}$$

where I used the shorthand notation $|1\rangle \equiv 1\,^3S_1$, $|2\rangle \equiv 2\,^3S_1$, $|P\rangle \equiv {}^3P_1$ for the unperturbed levels and the twiddle indicates the new eigenstates. The mixing angles can be calculated for small θ in lowest order perturbation theory

$$\theta_N = \frac{\langle N|\mathscr{H}_{NC}|P\rangle}{\sqrt{2M_N}\,(M_N - M_P)\sqrt{2M_P}}, \qquad N = 1, 2. \tag{2}$$

There are two diagrams which contribute — s and t channel exchange of Z_0 (Fig. V.1).

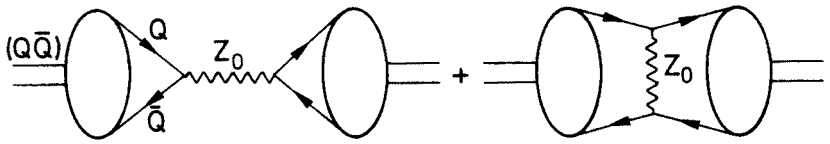

Fig. V.1

Their contribution is given by the amplitudes (a, b denotes the color indices)

$$A_s = \bar{v}_a\gamma_\mu(g_V + g_A\gamma_5)u_a \frac{1}{M_Z^2 - s}\,\bar{u}_b\gamma^\mu(g_V + g_A\gamma_5)v_b,$$

$$A_t = \bar{v}_a\gamma_\mu(g_V + g_A\gamma_5)v_a \frac{1}{M_Z^2 - t}\,\bar{u}_b\gamma^\mu(g_V + g_A\gamma_5)u_b. \tag{3}$$

The t exchange can be evaluated easier in the Fierz transformed version

$$A_t = \tfrac{1}{3}\,\bar{v}_a\gamma_\mu(g_V + g_A\gamma_5)u_a \frac{1}{M_Z^2 - t}\,\bar{u}_b\gamma^\mu(g_V + g_A\gamma_5)v_b \tag{4}$$

$$+\text{color octet terms}$$

$$+\text{scalar and tensor contributions.}$$

If one evaluates these amplitudes for quarkonia with masses up to 200 GeV, M_Z is far larger than the typical relative momentum and the t exchange can be approximated by an effective four fermion interaction with a relative contribution

$$A_t/A_s = \tfrac{1}{3}\,M_Z^2/(M_Z^2 - M^2). \tag{5}$$

The relevant transition amplitudes are evaluated as follows:

$$\langle N|\mathscr{H}_{NC}|P\rangle = \langle N|g_V V_{NC}|0\rangle\left(\frac{1}{M_Z^2 - M^2} + \tfrac{1}{3}\frac{1}{M_Z^2}\right)\langle 0|g_A A_{NC}|P\rangle$$

$$= f_V^N g_V M_N^2\left(\frac{1}{M_Z^2 - M^2} + \tfrac{1}{3}\frac{1}{M_Z^2}\right) f_A g_A M_P^2 \qquad N = 1, 2. \tag{6}$$

I shall use $M \approx M_{1,2} \approx M_P$ whenever possible.

V.3. The decay $2\,^3S_1 \to 1\,^3S_1+\gamma$

How could one observe this mixing? There is in fact one signal, namely, the direct decay $2\,^3S_1 \to 1\,^3S_1+\gamma$. It violates charge conjugation and is forbidden if weak interactions are ignored. In contrast to atomic physics, where neutral currents induce partiy violation, here a C violating decay is the signal to look for.

The relevant rates will first be calculated in a model independent way and expressed through the widths $\Gamma(\mathrm{P} \to 1+\gamma)$ and $\Gamma(2\mathrm{S} \to \mathrm{P}+\gamma)$, $f_{\mathrm{V}}^N, f_{\mathrm{A}}$ and the parameters of the Weinberg-Salam model. The mixing of P with 1 and 2 contributes and we shall see that the two amplitudes interfere always constructively. For superheavy states, the main contribution will come from the 2-P mixing due to their small mass difference in a nearly Coulombic potential.

The transition amplitude $\langle\tilde{2}|\mathscr{H}_{\mathrm{EM}}|\tilde{1}\rangle$ for the dipole transition can be easily evaluated for small mixing angles.

$$\langle\tilde{2}|\mathscr{H}_{\mathrm{EM}}|\tilde{1}\rangle = \theta_2\langle P|\mathscr{H}_{\mathrm{EM}}|1\rangle+\theta_1\langle 2|\mathscr{H}_{\mathrm{EM}}|\mathrm{P}\rangle \tag{8}$$

and the rate is given by

$$\Gamma(\tilde{2} \to \tilde{1}\gamma) = (M_2-M_1)^3\left(|\theta_2|\sqrt{\frac{\Gamma(\mathrm{P} \to 1+\gamma)}{(M_{\mathrm{P}}-M_1)^3}}+|\theta_1|\sqrt{\frac{\Gamma(2 \to \mathrm{P}+\gamma)}{(M_2-M_{\mathrm{P}})^3}}\right)^2. \tag{9}$$

The relative sign of the two contributions is given by the relative sign of

$$R_N(0)\int drrR_N(r)R_{\mathrm{P}}(r)/(M_N-M_{\mathrm{P}}) \tag{10}$$

for $N = 1$ and 2. It has been shown by A. Martin [III.8] that $R_N(0)\int drrR_N(r)R_P(r)$ is always relatively negative for $N = 1$ and 2. Together with the level ordering $M_2 > M_{\mathrm{P}} > M_1$ this implies constructive interference of the two contributions.

V.4. Numerical estimates and conclusions

To evaluate Eqs. (7, 9) one needs information about the wavefunctions of all three states under discussion. A realistic estimate would necessarily rely on extensive numerical calculations — and would still be untrustable because of the unknown short distance behaviour of the potential. However, once the various quarkonium levels and their radiative transitions have been experimentally observed, $f_{\mathrm{V}}^1, f_{\mathrm{V}}^2$ and the mass splitting are readily determined and the only missing quantity f_{A} can be calculated rather accurately.

To illustrate the order of magnitude, I will evaluate the ratio

$$\frac{\Gamma(2 \to 1+\gamma)}{\Gamma(2 \underset{\gamma Z}{\to} \mu^+\mu^-)} = 12\pi^2\alpha f_{\mathrm{A}}^2\,\frac{(1+\frac{1}{3}(M_Z^2-M^2)/M_Z^2)v_Q^2a_Q^2}{(\hat{e}_Q^2(M^2-M_Z^2)^2/M^4+v_Q^2a_\mu^2)}$$

$$\times\,\frac{M(M_2-M_1)^3\Gamma(\mathrm{P} \to 1+\gamma)}{(M_2-M_{\mathrm{P}})^2(M_{\mathrm{P}}-M_1)^3} \times \left(1+\frac{M_2-M_{\mathrm{P}}}{M_{\mathrm{P}}-M_1}\sqrt{\frac{\Gamma(2 \to \mathrm{P}+\gamma)(M_{\mathrm{P}}-M_1)^3\Gamma(1 \to \mu^+\mu^-)}{\Gamma(\mathrm{P} \to 1+\gamma)(M_2-M_{\mathrm{P}})^3\Gamma(2 \to \mu^+\mu^-)}}\right)^2 \tag{11}$$

for a quark with charge $e_Q = 2/3$ and with $\sin^2\theta_W = 1/4$ in a variety of simple potential models.

A Coulomb-like potential $V(r) = -\lambda/r$ determines the wavefunctions

$$R_1 = 2a^{-3/2}e^{-\varrho},$$

$$R_2 = 2^{-1/2}a^{-3/2}(\varrho/2-1)e^{-\varrho/2},$$

$$R_P = (24)^{-1/2}a^{-3/2}\varrho e^{-\varrho/2},$$

$$a^{-1} \equiv \lambda M/4, \quad \varrho \equiv r/a, \tag{12}$$

the couplings (see Eq. (III.12))

$$f_{V1}^2 = \frac{12}{\pi}\left(\frac{\lambda}{4}\right)^3, \quad f_{V2}^2 = \tfrac{1}{8}f_{V1}; \quad f_A^2 = \frac{3}{\pi}\left(\frac{\lambda}{4}\right)^5, \tag{13}$$

the mass difference between the nearly degenerate 2S, 1P and the 1S state

$$M_P - M_1 \approx M_2 - M_1 = \tfrac{3}{2}\left(\frac{\lambda}{4}\right)^2 M \tag{14}$$

and the transition rates for $\hat{e}_Q = 2/3$

$$\Gamma(2 \to P\gamma)/(M_2 - M_P)^3 = \tfrac{16}{3}a^2\alpha,$$

$$\Gamma(P \to 1\gamma)/(M_1 - M_P)^3 = (\tfrac{2}{3})^{13}a^2\alpha. \tag{15}$$

The mass splitting between the two nearly degenerate levels 2S and 1P is obtained from a linear correction $C \cdot r$ to the potential (Model 1)

$$M_2 - M_P = \langle Cr\rangle_2 - \langle Cr\rangle_P = C \cdot a \tag{16}$$

with $C = (0.4\ \text{GeV})^2$, or from a term which has a form similar to the one expected from fine structure splitting (Model 2)

$$M_2 - M_P = \left(\frac{\lambda}{4}\right)^4 \frac{M}{2} \cdot \delta, \tag{17}$$

where $\delta \approx O(1)$ is a set equal to one in the numerical calculations.

As a different alternative I use numerical results for charmonium ($\Gamma(1 \to \mu^+\mu^-)/\Gamma(2 \to \mu^+\mu^-) = 2.5$, $\Gamma(2 \to P+\gamma) = 34$ keV, $\Gamma(P \to 1+\gamma) = 320$ keV, $f_A^2 = 0.093$) and extrapolate them with the help of scaling laws for potentials of the form $V(r) \propto r^\nu$ as discussed in Chapter III.2. $\nu = 0$ (logarithmic potential) and $\nu = -1/2$ are chosen as Models 3 and 4.

The results, as displayed in Fig. V.2, are relatively insensitive to the choice of the model. The growth of the rates up to $M \approx 90$ GeV is of course mainly due to the increasing strength of weak interactions. Beyond the Z_0 pole there is destructive interference between s and t channel contribution, and even complete cancelation for $M = 2M_Z$.

In the optimal case of M between 80 GeV and 120 GeV the rates correspond to an overall branching ratio of roughly 10^{-6}. Only in the special case of $M \approx M_Z$ would the production rate be high enough to have any events at all — the back-ground problems however are probably prohibitive.

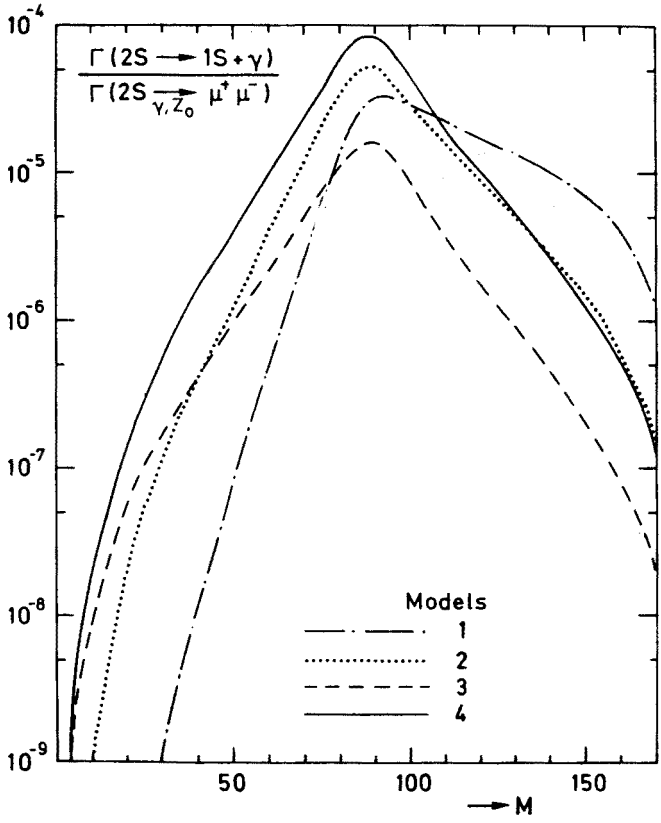

Fig. V.2

We conclude that even in mass regions, where weak interactions are extremely important for onium production and annihilation, their influence on the wave-functions is still negligibly small.

VI. CHARMONIUM PRODUCTION IN B-DECAYS

All the weak processes, which were discussed until now, were concerned with the interaction of heavy quarks and the gauge bosons and Higgs particle only. Strong interactions could be absorbed in the quarkonium potential. The following two chapters will deal with reactions where also light hadrons — in the language of QCD: light quarks and gluons — play an important role.

In this chapter I shall discuss charmonium production in B-meson decays. Originally the decay mode $B \to \psi K\pi$ was suggested by Fritzsch [1] as a particularly prominent and useful exclusive channel. Working in a naive quark model, in which the heavy b quark in the B-meson decays via $b \to \psi + s$ and neglecting any possible color suppression, he estimated a sizeable branching ratio for the inclusive decay of B into $K\psi$ of roughly 3%. In the framework of a more specific model Kühn, Nussinow and Rückl [2] calculated the relative and absolute branching ratios for the various charmonium channels and I will restate briefly the main results.

The effective weak hamiltonian for the decay $b \to c\bar{c}s$ takes the form [3]:

$$\mathscr{H}_{\text{eff}} = v \frac{G_F}{\sqrt{2}} \left[\frac{C_+ + C_-}{2} (\bar{c}_a b_a)(\bar{s}_b c_b) + \frac{C_+ - C_-}{2} (\bar{s}_a b_a)(\bar{c}_b c_b) + \text{h.c.} \right], \tag{1}$$

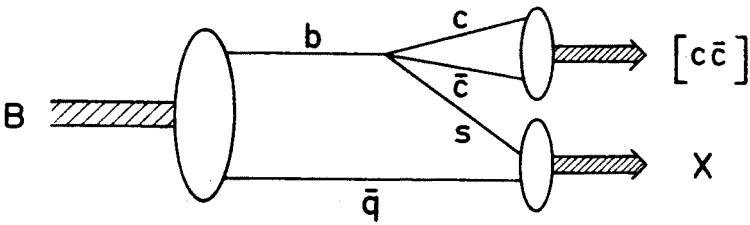

Fig. VI.1

where $(\bar{q}_a q'_a)$ stands for the sum $\sum_a (\bar{q}'_a \gamma_\mu (1-\gamma^5) q'_a)$ and v for the relevant combination of mixing angles. $C_+ = C_- = 1 (C_+ = 1.4,\ C_- = 0.85)$ in the quark model without (with) hard gluon corrections. In order to obtain the amplitude for the decay $b \to [c\bar{c}]s$, (Fig.VI.1) where $c\bar{c}$ denotes a color singlet charmonium state, one considers the Fierz transformed operator and takes only the color singlet term

$$\langle s[c\bar{c}]|\mathscr{H}_{\text{eff}}|b\rangle = v \frac{G_F}{\sqrt{2}} C \langle s|(\bar{s}_a b_a)|b\rangle \langle [c\bar{c}]|(\bar{c}_b c_b)|0\rangle. \tag{2}$$

The coefficient $C = (2C_+ - C_-)/3$ is equal 1/3(0.1) in the model without (with) gluon corrections. On the other hand Fritzsch argued that this color suppression might not be operative due to color neutralization by soft gluons, which would then imply $C = 1$. All the branching ratios into charmonium states will be proportional to C^2 and thus a measurement of their decays would determine C. In the following we shall put $C \cdot v = 1$.

The matrix element $\langle [c\bar{c}]|\bar{c}\gamma_\mu(1-\gamma_5)c|0\rangle$ can now be evaluated in a straightforward manner, as described in Appendix B. One obtains

$$\Gamma(b \to s + \psi) = \frac{G_F^2 m_b^5}{192\pi^3} \frac{81\pi}{4\alpha^2} M_\psi \Gamma(\psi \to e^+ e^-) \frac{\sqrt{\Delta(m_b^2, m_s^2, M_\psi^2)}}{m_b^8}$$

$$\times [(m_b^2 - m_s^2)^2 - 2M_\psi^4 + M_\psi^2 (m_b^2 + m_s^2)], \tag{3}$$

$$\Gamma(b \to s+\eta_c) = \frac{G_F^2 m_b^5}{192\pi^3} \frac{81\pi}{4\alpha^2} M_\psi \Gamma(\psi \to e^+e^-) \frac{\sqrt{\Delta(m_b^2, m_s^2, M_\psi^2)}}{m_b^8}$$

$$\times [(m_b^2 - m_s^2)^2 - M_\psi^2(m_b^2 + m_s^2)] \tag{4}$$

$$\Gamma(b \to s+\chi_1) = \frac{G_F^2 m_b^5}{192\pi^3} 12\pi^2 M_\chi^2 f_A^2 \frac{\sqrt{\Delta(m_b^2, m_s^2, M_\chi^2)}}{m_b^8}$$

$$\times [(m_b^2 - m_s^2)^2 - 2M_\chi^4 + M_\chi^2(m_b^2 + m_s^2)] \tag{5}$$

and f_A is given in Chapter III.

TABLE VI.I

Reduced partial widths for $b \to [c\bar{c}]+s$ (Note that we have put $C = v = 1$)

State	Mass [GeV]	$\Gamma_{e^+e^-}$ [keV]	$\Gamma(b \to [c\bar{c}]+s)$ [GeV/C^2v^2]	
			$m_b = 4.8$ GeV	$m_b = 5$ GeV
η_c	3.0	—	1.54×10^{-11}	1.83×10^{-11}
J/ψ	3.095	4.8	2.70×10^{-11}	3.31×10^{-11}
P_c/χ_1	3.510	—	7.15×10^{-12}	9.30×10^{-12}
ψ'	3.686	2.1	8.10×10^{-12}	1.10×10^{-11}
ψ''	3.771	0.37	1.29×10^{-12}	1.80×10^{-12}

The reduced partial widths $\Gamma(b \to [c\bar{c}]+s)$ for all charmonium states are listed in Table VI.I. Note that in order to obtain the actual partial widths one has to multiply these values by C^2v^2. The corresponding branching ratios (modulo C^2) are listed in Table VI.II. They follow from the partial widths of Table VI.I and the total width estimated in the naive quark model:

$$\Gamma(B \to \text{all}) \approx 2.7v^2 \frac{G_F^2 m_b^5}{192\pi^3} = v^2 \times 0.16 \text{ eV}. \tag{6}$$

TABLE VI.II

Branching ratios for $B \to [c\bar{c}]+X$ derived from the decay $b \to [c\bar{c}]+s$ with $m_b = 4.8$ GeV

$[c\bar{c}]$	$B(B \to [c\bar{c}]+X)$
η_c	$0.10\,C^2$
J/ψ	$0.17\,C^2$
P_c/χ_1	$0.05\,C^2$
ψ'	$0.05\,C^2$
ψ''	$0.01\,C^2$

Let me conclude with some comments:

a) The relative production rate for the various charmonium states is independent of C^2 and v^2 and ψ is clearly dominant

$$\eta_c : J/\psi : P_c/\chi_1 : \psi' = 0.57 : 1 : 0.27 : 0.31$$

b) Decays into χ_0, χ_2 and $^1P_1$ are forbidden.

c) Even if $C = 1/3$ as expected from the bare Hamiltonian (Eq. (1)), one finds a surprisingly large branching ratio for $B \to J/\psi + X$ of roughly 2%. However the QCD modified Hamiltonian with $C = 0.1$ leads to a disastrously small result.

d) In the model the light quark is treated as spectator. The mass of the recoiling system X is completely fixed by the mass of the charmonium state

$$M_X = \sqrt{M_B(M_B - m_b + m_s^2/m_b) + M_{[c\bar{c}]}^2(1 - M_B/m_b)}\,. \tag{7}$$

This leads to a rather small result for M_X of $\sim 1 - 1.2$ GeV and thus one may hope that final states with low multiplicity constitute a sizeable fraction of X.

VII. NEUTRINO PRODUCTION OF CHARMONIUM[17]

VII.1. General remarks

Neutrino production of vector and axial vector states has been proposed already some time ago by C. A. Piketty and L. Stodolsky [1]. The existence of neutral current couplings, as predicted by the Weinberg Salam model, allows in particular diffractive production of neutral states like ϱ, ω and φ or their axial analogs. With the discovery of charmonium the corresponding reactions for ψ and χ_1 production have received considerable attention [2–5]. In this chapter I will discuss and compare various models, their similarities and limits of applicability. In contrast to the previous sections the dynamics of light hadrons will be highly important. The production occurs off a nucleon target (N) and thus hadronic cross sections and the gluon distribution play an essential role. In fact the reaction allows us to measure the hadronic cross sections of ψ and χ_1, if we take the weak couplings for granted. Conversely we can in principle determine g_V, if we use the hadronic cross sections, as determined in muo-production.

The two models, which I will discuss in parallel, are the vector dominance model [1–4] and the Z_0-gluon-fusion model [4–5]. In the VDM (Fig. VII.1) one assumes that the virtual Z_0 with momentum q couples to ψ and χ_1 proportional to g_V and g_A, respectively. The charmonium then scatters diffractively off the target and can then be observed through its characteristic decay modes. In order that this intuitive picture makes sense one requires that the virtual ψ is formed before it interacts with the target, or in other words, that it "lives" longer than $T \approx 1/m_\pi$. This can be translated into an inequality[18] for ν and Q^2.

$$\Delta E = \sqrt{M_\psi^2 + Q^2 + \nu^2} - \nu \approx (M_\psi^2 + Q^2)/2\nu < m_\pi \tag{1}$$

[17] This chapter is partly based on work done in collaboration with R. Rückl [4].

[18] The kinetic variables are defined in the usual way: $Q^2 = -q^2$, $\nu = q \cdot p/M_N$; $X = Q^2/2M_N$; $y = \nu/E$.

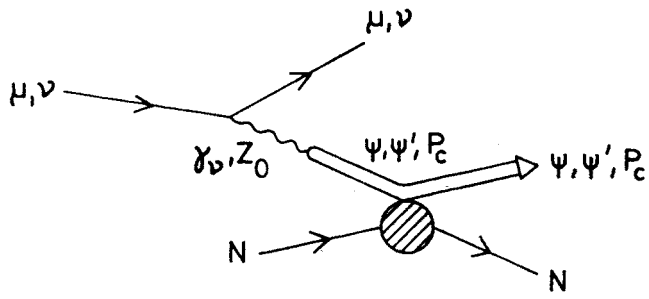

Fig. VII.1

or alternatively $\sqrt{|t_{\min}|} < m_\pi$. Thus the process may be soft or pointlike, depending on the specific kinematical situation.

The alternative model (Fig. VII.2) is based on QCD and the notion of local duality [6]. The virtual Z_0 fuses with a gluon of the nucleon and produces a $c\bar{c}$ pair with invariant mass Δ. If Δ is within the interval $2m_C < \Delta < 2m_D$, i.e., below the threshold for open charm production, it is furthermore assumed that the $c\bar{c}$ pair converts into the various charmonium states with roughly equal probabilities, which add up to one, and in particular into ψ with a probability $1/n = 1/6$. Given Δ^2, Q^2 and ν, the gluons momentum fraction ξ can easily be calculated

$$\xi = \frac{\Delta^2+Q^2}{2M_N\nu} \approx \frac{M_\psi^2+Q^2}{2M_N\nu} . \tag{2}$$

From Eqs. (1, 2) one deduces that hard gluons ($\xi \gtrsim 0.1$) are involved if short time scales play an important role, and it is this region where one expects that lowest order perturbative QCD should be valid. In the complementary region of small ξ rescattering effects could be important and could strongly influence the results.

In the following Section VII.2 I will briefly contrast the two models in the case of photo- and muo-production — where the predictions are rather similar, and tune the free parameters with the help of existing data. In Section VII.3 I shall contrast the strikingly different predictions of the two models for neutrino production of ψ. Section VII.4 is concerned with the contribution of other charmonium states and the conclusions.

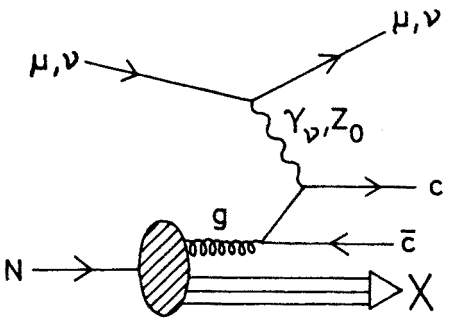

Fig. VII.2

VII.2. Photo- and Muo-production of ψ

Experimentally a large amount of data for photoproduction of ψ has been accumulated in the energy region between 20 and 200 GeV [7–9]. Muo- and (virtual) photo- production are related by a simple flux factor

$$\frac{d\sigma^{\mu}}{dvdQ^2} = \Gamma\sigma^{\gamma^*}(v, Q^2), \tag{3}$$

where

$$\Gamma = \frac{\alpha}{2\pi}\,\frac{v-Q^2/2M_N}{E^2Q^2(1-\mathscr{E})}, \qquad \mathscr{E} = \frac{4E(E-v)-Q^2}{2(E^2+(E-v)^2)+Q^2}.$$

In general, one has contributions from transverse and longitudinal photons

$$\sigma^{\gamma} = \sigma^{T}+\mathscr{E}\sigma^{L}. \tag{4}$$

Muo-production is dominated by low Q^2 and we will therefore ignore the longitudinal contribution.

In the VDM, production by offshell photons is related to the real photo-production cross section $\sigma^{\gamma}(v)$ by

$$\sigma^{\gamma^*}(v, Q^2) = \sigma^{\gamma}(v)\,(1+Q^2/M_{\psi}^2)^{-2}. \tag{5}$$

The expectations of vector dominance for the Q^2 dependence are reasonably well confirmed by the data (Fig. VII.3).

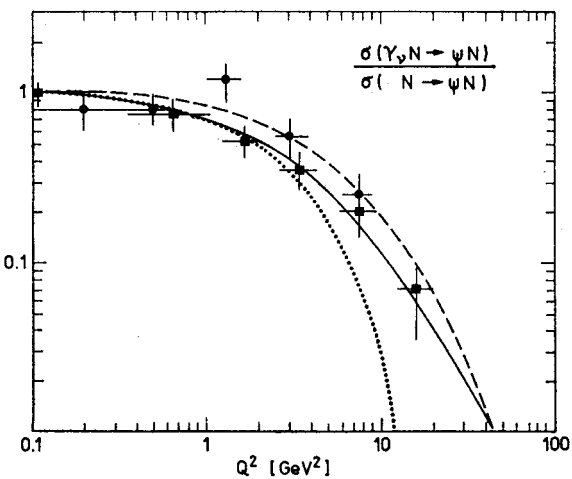

Fig. VII.3. Off-shell-behaviour of the virtual photoproduction of ψ. The data are taken from Ref. VII. [8] (●) and Ref. VII [9] (■). The full line is the VDM parametrization Eq. (3) with $M = 2.4$ GeV, the dotted ($\nu = 20$ GeV) and dashed ($\nu = 100$ GeV) curves are predictions of the fusion model

The model makes no prediction for the energy dependence of the cross section. The experimental results are displayed in Fig. VII.4, together with the phenomenological parametrization

$$\sigma^{\gamma}(\nu) = 30 \text{ nb} \times \exp\left[-20 \text{ GeV}/(\nu - 6 \text{ GeV})\right]. \tag{6}$$

With this input and Eqs. (3), (5) one obtains the integrated elastic ψ rate in muo-production as function of the muon energy, as shown in Fig. VII.5, and consistent with the experimental result at $E_{\mu} = 209$ GeV : $\sigma(\mu N \to \mu N \psi) = 0.67 \pm 20$ nb. This agreement is not surprising, since we have fitted $\sigma^{\gamma^*}(\nu)$ to data at $Q^2 = 0$ and muo-production in turn is dominated by low Q^2.

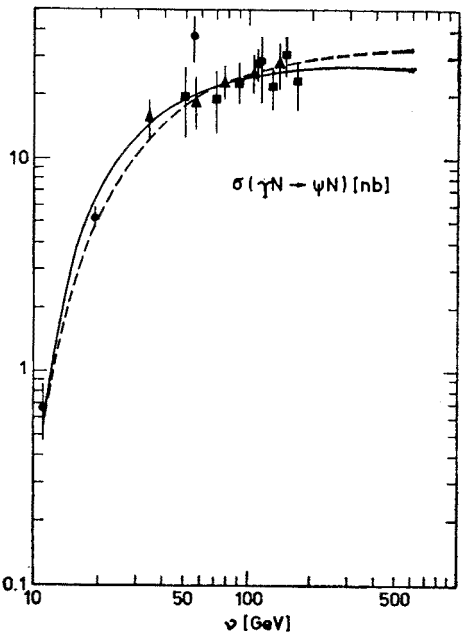

Fig. VII.4. Energy dependence of the photoproduction of ψ. The data for real photons are taken from Ref. VII. [7] (●), the data for virtual photons extrapolated to $Q^2 = 0$ are taken from Ref. VII. [8] (▲) and Ref. VII. [9] (■). The full curve is the parametrization described in the text, the dashed curve is a fusion model prediction

In the competing QCD model the cross section can be calculated in terms of the gluon distribution $G(\xi)$, the quark mass m_c and the normalization $1/n$

$$\sigma^{\gamma^*}(\nu, Q^2) = \frac{1}{n} \int_{\frac{4m_c^2 + Q^2}{2M_N \nu}}^{\frac{4m_D^2 + Q^2}{2M_N \nu}} d\xi G(\zeta) \sigma(\gamma^* g \to c\bar{c}) \tag{7}$$

and $\sigma(\gamma^* g \to c\bar{c})$ can be evaluated in a straightforward manner [10–13]. If we use the nonrelativistic approximation $\beta = \sqrt{1-m_c^2/m_D^2} \ll 1$, the result becomes more transparent [4], can be compared easily with VDM and cast into the form of Eq. (3) with

$$\sigma^{\gamma^*}(\nu, Q^2) = \frac{1}{n}\,\frac{\pi}{3}\,\frac{4}{9}\,\alpha\alpha_s\,\frac{m_D^2\left(1-\dfrac{m_c^2}{m_D^2}\right)^{3/2}}{m_c^4\left(1-\dfrac{Q^2}{2M_N\nu}\right)}\,\frac{\xi G(\xi)}{\left(1+\dfrac{Q^2}{4m_c^2}\right)^2}$$

$$\xi = \frac{M_\psi^2+Q^2}{2M_N\nu}. \tag{8}$$

In the region under consideration this form approximates the exact result up to $\sim 10\%$ and exhibits a number of interesting features:

a) As long as $\xi G(\xi) \approx$ const, i.e., for small ξ (limited Q^2, large ν) the VDM propagator is reproduced and governs the Q^2 behaviour. For medium and small ν the Q^2 dependence gets steeper due to the additional decrease of $\xi G(\xi)$. This can be seen from Fig. VII.3, which shows the Q^2 dependence of the exact result for $\nu = 20$ and 100 GeV.

b) The longitudinal cross section vanishes in the nonrelativistic approximation.

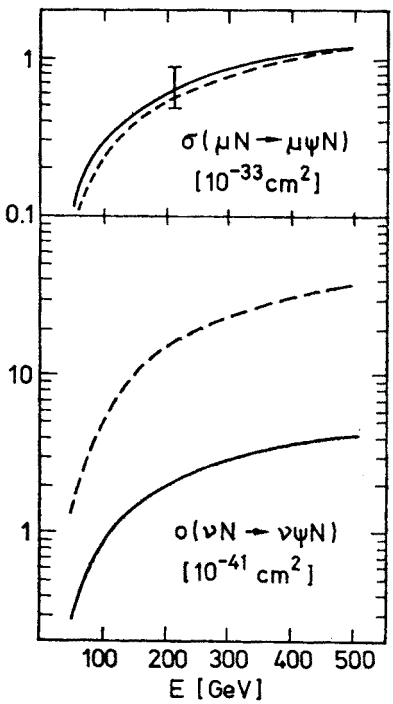

Fig. VII.5. Diffractive, elastic ψ production rates. The full curves are VDM predictions, the dashed curves are fusion model predictions. The data point is from Ref. VII. [8]

c) The energy dependence of $\sigma^{\gamma}(\nu)$ is largely determined by the gluon structure function, the normalization by the quark mass, α_s and $1/n$. These unknown quantities introduce a substantial flexibility and this explains the large difference between different theoretical predictions [10–13]. Still it is remarkable that the "canonical" choices $m_c = 1.5$ GeV, $\alpha_s = 0.4$, $\xi G(\xi) = (1-\xi)^5$ and $1/n = 1/6$ are in rather good agreement with the experimental results, as shown in Figs. VII.3 and 4.

d) The VDM predicts dominant production of the vector states ψ and ψ'. Local duality, however, taken literally predicts comparable rates for all charmonium states in all production processes. To account for a reaction dependent relative weight, one has to introduce additional free parameters into the model.

VII.3. Neutrino production

After having fixed the parameters of the models, let us turn to the original problem, namely, neutrino production of charmonium. In the VDM the conversion of muon into neutrino cross section is straightforward. In total, one has to replace $e^4 e_c^2/2Q^4$ in Eq. (3) by $(g_V^2+g_A^2)g_V^{c2}/M_Z^4$. In the standard model the conversion reads

$$\frac{d\sigma^{\nu}}{d\nu dQ^2} = \frac{9G_F^2(1-\frac{8}{3}\sin^2\theta_W)^2}{128\pi^2\alpha^2}\, Q^4 \Gamma \sigma^{\gamma^*}(\nu, Q^2). \tag{9}$$

From that, and the parametrization of σ^{γ^*} given in the last section, one finds the integrated, diffractive, elastic ψ production as displayed in Fig. VII.4 as a function of the neutrino energy. Note that the integration extends beyond the region where the diffractive VDM is strictly valid.

In the fusion model, on the other hand, one has to compute the cross section for the subprocess $Z_0 g \to c\bar{c}$ (Fig. VII.2) and to fold in the gluon structure function. The qualitative features can be discussed more easily if we use again the nonrelativistic approximation. Then

$$\frac{d\sigma^{\nu}}{d\nu dQ^2} \simeq \frac{9G_F^2(1+(1-\frac{8}{3}\sin^2\theta_W)^2)}{128\pi^2\alpha^2}\, Q^4 \Gamma$$

$$\times \left[1 + \frac{1}{1+(1-\frac{8}{3}\sin^2\theta_W)^2}\, \frac{16m_c^2}{Q^2}\, \frac{E(E-\nu)}{E^2+(E-\nu)^2}\right] \sigma^{\gamma^*}(\nu, Q^2) \tag{10}$$

and $\sigma^{\gamma^*}(\nu, Q^2)$ is given by Eq. (8).

Several comments ought to be made:

a) If we compare this with the VDM result, we realize that vector and axial coupling both contribute to ψ production — and in fact g_A^2 dominates the rate.

b) The axial coupling induces a sizeable longitudinal cross section, which was absent in muo-production.

c) Whereas VDM allows the production of ψ, ψ' and χ_1 only, with couplings proportional to g_V^2 and g_A^2 respectively, in the QCD-fusion model also the production of the other states, e.g., η_c, χ_0 and χ_2, is possible and should occur with comparable strength.

Using for α_s, m_c, n and $\xi G(\xi)$ the same values as previously in photo-production and furthermore $\sin^2 \theta_W = 0.23$, one obtains the integrated, elastic ψ rate as plotted in Fig. VII.4. As expected from the large axial contribution, the QCD result is larger by a factor 5–8. However one should keep in mind that the VDM estimate was based on low Q^2 information only, whereas the large Q^2 region contributes significantly in neutrino reactions. Longitudinal contributions, which we have ignored, could be important.

VII.4 Other charmonium states

Both models can be extended to estimate the contribution of other charmonium states. In the VDM the evaluation is straightforward. For the Z_0-charmonium couplings we use $(f'_V/f_V)^2 = 0.4$ for ψ' and $(f_A/f_V)^2 = 0.4$ for χ_1 as discussed in Chapter III. Assuming furthermore equal hadronic cross sections and using the bound state masses in the VDM form factor, one obtains [4]

$$\psi : \psi' : \chi_1 = 1 : 0.6 : 3.3. \tag{11}$$

All other charmonium states are forbidden. Considering the relatively large branching ratio for $\chi_1 \to \psi\gamma$ of roughly 30%, we obtain an indirect contribution to ψ production, which is as important as the direct channel.

The Z_0-gluon-fusion model does not give a clear and convincing recipe to evaluate the relative weights. However, there is no reason to expect an extremely prominent χ_1 signal, but rather roughly equal production of the various states.

Is there a chance to detect and identify this rather large χ_1 signal? There are two signatures which might help:

a) The photon from the cascade decay is rather soft (~ 0.4 GeV) in the χ_1 rest frame. In the laboratory frame it has an energy ranging from 0 up to $2 \times 0.4\,\text{GeV} \times \frac{\nu}{M_\chi}$ and thus could eventually be detected.

b) The angular distribution of the decay products is quite different for direct and indirect ψ production. Assuming s channel helicity conservation and neglecting longitudinal contributions, one obtains the muons angular distribution in the ψ rest frame from directly produced ψ

$$\frac{dN}{d\cos(\vec{e}_\mu \vec{e}_Z)} \propto (1 + \cos^2(\vec{e}_\mu \vec{e}_Z)), \tag{12}$$

where $\vec{e}_\mu$ and $\vec{e}_Z$ are unit vectors in the momentum direction of the muon and the Z_0. Diffractive χ_1 production with subsequent cascade decay $\chi_1 \to \psi\gamma \to \gamma\mu^+\mu^-$ leads to the following angular distribution for muons and photons:

$$dN \propto (1 - \cos(\vec{e}_\mu \vec{e}_Z) \cos(\vec{e}_Z \vec{e}_\gamma) \cos(\vec{e}_\gamma \vec{e}_\mu)) d(\text{LIPS}) \tag{13}$$

which in turn implies muon and photon distributions of the form

$$\frac{dN}{d\cos(\vec{e}_\mu \vec{e}_Z)} \propto (1-\tfrac{1}{3}\cos^2(\vec{e}_\mu \vec{e}_Z)), \tag{14}$$

$$\frac{dN}{d\cos(\vec{e}_\gamma \vec{e}_Z)} \propto (1-\tfrac{1}{3}\cos^2(\vec{e}_\gamma \vec{e}_Z)). \tag{15}$$

Thus direct and indirect production could be experimentally distinguished through the muon distribution.

Let me summarize:

a) Diffractive neutrino production of charmonium offers the unique chance of measuring the couplings of the vector and axial part of the neutral current to charmed quarks.

b) The reaction allows furthermore to discriminate between the VDM and the Z_0-gluon fusion model, which give rather similar predictions for photo- and muo-production.

c) For a neutrino energy of 100 GeV VDM gives $\sigma(\nu N \to \nu\psi N) \approx 10^{-41}$ cm^2, and the fusion model $\approx 5\times 10^{-41}$ cm^2. If inelastic charmonium production is of the same order as the elastic rate, as observed in muo-production, one has to multiply the result by a factor two. In VDM one has to multiply by another factor two to account for the large amount of indirect production through χ_1. Thus one obtains an inclusive rate for ψ's of roughly 10^{-40} cm^2 in the fusion model, and 0.4×10^{-40} cm^2 in the VDM. These theoretical results come already rather close to the experimental upper limit [14] of 2.2×10^{-40} cm^2.

I am indebted to many colleagues for helpful discussions on "Weak Interactions of Quarkonia". In particular I would like to thank I. Bigi, B. Guberina, J. Kaplan, S. Nussinov, R. D. Peccei, R. Rückl, H. Schneider and E. G. O. Safiani for their invaluable contributions. Finally I want to express my gratitude to the organizers of the XX Cracow School of Theoretical Physics for their kind hospitality.

APPENDIX A

The standard model

For convenience and easy reference I list the electroweak couplings of leptons and hadrons as predicted in the standard model. The neutral current coupling is given by

$$\mathcal{L}_{NC} = \sum_f \bar{f}\gamma_\mu(g_V^f + g_A^f\gamma_5)f Z^\mu \tag{1}$$

with coupling constants

$$g_V^f = \frac{g}{4\cos\theta_W}(2I_3^f - 4\hat{e}_f \sin^2\theta_W), \qquad g_A^f = -\frac{g}{4\cos\theta_W} 2I_3^f, \tag{2}$$

where $\hat{e}_f$ is the fermion charge in units of e, and I_3^f is the third component of the weak

isospin:

$$I_3^f = \begin{cases} \frac{1}{2} & f = e, \mu, \tau, \quad u, c, t \\ -\frac{1}{2} & f = \nu_e, \nu_\mu, \nu_\tau, \quad d, s, b. \end{cases} \tag{3}$$

In the limit of an effective four fermion interaction it is convenient to use

$$\frac{g}{4 \cos \theta_W M_Z} = \left(\frac{G_F}{2\sqrt{2}}\right)^{1/2}. \tag{4}$$

To compare neutral current and electromagnetic interactions at high energies, it is useful to introduce the ratios

$$a \equiv g_A/e = -\frac{2I_3}{e}\left(\frac{M_Z^2 G_F}{2\sqrt{2}}\right)^{1/2} = -2I_3/(4 \sin\theta_W \cos\theta_W),$$

$$v \equiv g_V/e = (2I_3 - 4\hat{e} \sin^2\theta_W)/e\left(\frac{M_Z^2 G_F}{2\sqrt{2}}\right)^{1/2} = (2I_3 - 4\hat{e} \sin^2\theta_W)/(4 \sin\theta_W \cos\theta_W). \tag{5}$$

The relative strengths (for $q^2 \ll M_Z^2$, also the absolute strengths) of the axial couplings for quarks and leptons and also q_V^ν are independent of the Weinberg angle

$$g_A^{d,\nu} = -g_A^{u,e} = -g_V^\nu = g/4 \cos\theta_W = M_Z\left(\frac{G_F}{2\sqrt{2}}\right)^{1/2}. \tag{6}$$

The vector couplings get particularly simple for $\sin^2\theta_W = 1/4$. g_V^e vanishes and

$$g_V^u = \tfrac{1}{3}\, g/(4 \cos\theta_W),$$

$$g_V^d = -\tfrac{2}{3}\, g/(4 \cos\theta_W). \tag{7}$$

The charged current interactions are of course constructed such that they reproduce the standard V-A theory in the low energy limit

$$\mathscr{L}_{CC} = \left(M_W^2 \frac{G_F}{\sqrt{2}}\right)^{1/2} \left(\sum_{ff'} \bar{f}\gamma_\mu(1-\gamma_5)f'\right) W^\mu + \text{h.c.} \tag{8}$$

and we can relate the masses of the intermediate bosons and G_F

$$M_Z^2 \frac{G_F}{\sqrt{2}} = \frac{M_W^2}{\cos^2\theta_W} \frac{G_F}{\sqrt{2}} = \frac{4\pi\alpha}{8 \sin^2\theta_W \cos^2\theta_W} = 2 \times 4\pi\alpha a^2. \tag{9}$$

For $\sin^2\theta_W = 0.23$ one finds $M_Z = 89.75$ GeV and $M_W = 78.76$ GeV. The mass of Z_0 is used to define scaled masses for the boundstate, the Higgs meson and a scaled width

$$\mu \equiv M/M_{Z_0}, \quad \mu_H \equiv M_H/M_{Z_0}, \quad \mu_\Gamma \equiv \Gamma/M_{Z_0}.$$

APPENDIX B

Annihilation of onia

Suppose the amplitude for the annihilation of a free fermion and antifermion with momenta ff and spins $s\bar{s}$ is given by[12]

$$\mathcal{M} = \bar{v}(\vec{f}, \bar{s})\mathcal{O}u(f, s), \tag{1}$$

$\mathcal{O}$ denotes some Dirac operator and may depend on additional variables. For example $\mathcal{O}$ would be γ_μ or $\gamma_\mu\gamma_5$, if the annihilation went through a vector or axial vector current. If it goes through two virtual photons with momenta p_1, p_2 and polarizations $\mathscr{E}_1$, $\mathscr{E}_2$ then

$$\mathcal{O} = \frac{1}{i}\left[(-ie\gamma\mathscr{E}_2)\frac{i}{\gamma f-\gamma p_1-m}(-ie\gamma\mathscr{E}_1)+(-ie\gamma\mathscr{E}_1)\frac{i}{\gamma f-\gamma p_2-m}(-ie\gamma\mathscr{E}_2)\right]. \tag{2}$$

If fermion and antifermion can be treated in the non-relativistic approximation and are bound in a state $\psi_{s\bar{s}}(\vec{q})$, then the amplitude in the bound-state rest frame is given by

$$A = \sqrt{\frac{1}{m}}\int\frac{d\vec{q}}{(2\pi)^{3/2}}\,\psi_{s\bar{s}}(\vec{q})\bar{v}(\vec{f}, \bar{s})\mathcal{O}u(f, s),$$

$$f-\bar{f} = 2q = (0, 2\vec{q}), \quad f+\bar{f} = Q = (M, \vec{0}),$$

$$\sum_{s\bar{s}}\int d\vec{q}|\psi_{s\bar{s}}(\vec{q})|^2 = 1 \tag{3}$$

M = mass of the bound-state, m = fermion mass.

It is convenient to convert the matrix element $\bar{v}\mathcal{O}u$ into a trace of γ matrices and to combine the fermions into singlet and triplet states

$$\sum_{s\bar{s}}\bar{v}(\vec{f}, \bar{s})\mathcal{O}u(f, s)\,\langle\tfrac{1}{2}, s; \tfrac{1}{2}, \bar{s}|S, S_z\rangle$$

$$= \frac{1}{\sqrt{E_f+m}}\frac{1}{\sqrt{E_f+m}}\mathrm{Tr}\left[\mathcal{O}(m+\gamma f)\frac{M+\gamma p}{2M\sqrt{2}}\Pi_{Ss_z}(m-\gamma\bar{f})\right] \tag{4}$$

with

$$\Pi_{00} = -\gamma_5, \quad \Pi_{1,s_z} = -\gamma\mathscr{E}_{s_z},$$

where $\mathscr{E}_{s_z}$ denotes the spin polarization vector.

---

[19] We use the conventions of Bjorken-Drell. Our spinor normalization, however, is different: $u = \sqrt{2m}\,u_{BD}$.

Since we are only interested in terms up to first order in q/m, the amplitudes can be rewritten in the form

$$A = M^{-3/2} \int \frac{d\vec{q}}{(2\pi)^{3/2}} \psi_{LM}(\vec{q}) \langle L, MSS_Z | JJ_Z \rangle \operatorname{Tr} [\mathcal{O}(m+\gamma f)\Pi_{SS_Z}(m-\gamma \bar{f})]$$

$$\equiv \int \frac{d^4q}{(2\pi)^4} \operatorname{Tr} \mathcal{O}(q)\chi(Q, q). \tag{5}$$

We expand the trace up to terms linear in the relative momentum q and define

$$\mathcal{O}(0) \equiv \mathcal{O}(q = 0), \quad \mathcal{O}^\alpha \equiv \frac{\partial}{\partial q_\alpha} \mathcal{O}(q)|_{q=0}. \tag{6}$$

Using furthermore

$$\int \frac{d\vec{q}}{(2\pi)^{3/2}} \psi_{00}(\vec{q}) = \frac{1}{\sqrt{4\pi}} R_S(0),$$

$$\int \frac{d\vec{q}}{(2\pi)^{3/2}} q_\mu \psi_{1M}(\vec{q}) = -i \sqrt{\frac{3}{4\pi}} R'_P(0) \mathcal{E}_\mu^{(M)} \tag{7}$$

for S and P states, respectively, one can now perform the integral. For S waves one obtains

$$A = \tfrac{1}{2} \frac{1}{\sqrt{M}} \frac{1}{\sqrt{4\pi}} R_S(0) \operatorname{Tr} [\mathcal{O}(0)\,(M+Q)\Pi_{SS_Z}], \tag{8}$$

where $\Pi_{SS_z} = -\gamma_5$ for $^1S_0$ and $\Pi_{SS_z} = -\gamma \mathcal{E}$ for $^3S_1$.

For P waves one obtains in general

$$A = -\tfrac{1}{2} \frac{i}{\sqrt{M}} \sqrt{\frac{3}{4\pi}} R'_P(0) \langle LmSS_Z | JJ_Z \rangle \operatorname{Tr} \left[\mathcal{O}^\mu \mathcal{E}_\mu^{(m)} (M+\gamma Q)\Pi_{SS_Z} \right.$$

$$\left. + \frac{1}{M} \mathcal{O}(0)\,(\gamma \mathcal{E}^{(m)} \Pi_{SS_Z}(M-Q) + (M+Q)\Pi_{SS_Z} \gamma \mathcal{E}^{(m)}) \right] \tag{9}$$

and particularly for $^1P_1$

$$A(^1P_1) = \frac{i}{\sqrt{M}} \tfrac{1}{2} \sqrt{\frac{3}{4\pi}} R'_P(0) \operatorname{Tr} \left[\left(\mathcal{O}^\mu \mathcal{E}_\mu - \frac{2}{M} \mathcal{O}(0) \gamma \mathcal{E} \right) (M+\gamma Q)\gamma_5 \right]. \tag{10}$$

For triplet P states one has to combine $\vec{L}$ and $\vec{S}$ to $\vec{J}$ with the help of

$$\mathcal{E}_\mu^{(S_Z)} \mathcal{E}_\nu^{(m)} \langle 11 S_Z m | 00 \rangle = \frac{1}{\sqrt{3}} \left(g_{\mu\nu} - \frac{Q_\mu Q_\nu}{M^2} \right), \tag{11}$$

$$\mathscr{E}_{\mu}^{(S_z)}\mathscr{E}_{\nu}^{(m)}\langle 11S_Zm|1J_Z\rangle = -\frac{i}{M}\frac{1}{\sqrt{2}}\varepsilon_{\mu\nu}^{\alpha\beta}Q_{\alpha}\mathscr{E}_{\beta}(J)_z, \tag{12}$$

$$\mathscr{E}_{\mu}^{(S_z)}\mathscr{E}_{\nu}^{(m)}\langle 11S_Zm|2J_Z\rangle = \mathscr{E}_{\mu\nu}(J_Z) \tag{13}$$

and obtains finally

$$A(^3P_0) = i\sqrt{\frac{1}{4\pi M}}\,R'_P(0)\ \mathrm{Tr}\left[\mathscr{O}^{\mu}\left(\gamma_{\mu}+\frac{Q_{\mu}}{M}\right)(\gamma Q-M)/2+3\mathscr{O}(0)\right], \tag{14}$$

$$A(^3P_1) = -\sqrt{\frac{3}{8\pi M}}\,R'_P(0)\varepsilon_{\alpha\beta\gamma\delta}\frac{Q^{\gamma}}{M}\mathscr{E}^{\delta}\,\mathrm{Tr}\left[\mathscr{O}^{\alpha}\gamma^{\beta}(\gamma Q-M)/2-\mathscr{O}(0)\gamma^{\alpha}\gamma^{\beta}\frac{\gamma Q}{M}\right], \tag{15}$$

$$A(^3P_2) = i\sqrt{\frac{3}{4\pi M}}\,R'_P(0)\mathscr{E}_{\alpha\beta}\,\mathrm{Tr}\,[\mathscr{O}^{\alpha}\gamma^{\beta}(\gamma Q-M)/2]. \tag{16}$$

REFERENCES

1. Introduction

[1] T. Appelquist, H. D. Politzer, *Phys. Rev. Lett.* **34**, 43 (1975).
[2] V. A. Novikov et al., *Phys. Rep.* **41C**, 1 (1978).
[3] C. Quigg, J. L. Rosner, *Phys. Rep.* **56C**, 167 (1979).
[4] H. Grosse, A. Martin, *Phys. Rep.* **60C**, 341 (1980).
[5] S. Weinberg, *Phys. Rev. Lett.* **19**, 1264 (1967).
[6] A. Salam, in *Elementary Particle Physics*, ed. by N. Svartholm, Stockholm 1968, p. 367.
[7] S. L. Glashow, J. Iliopoulos, L. Maiani, *Phys. Rev.* **D2**, 1285 (1970).

Chapter II

[1] I. Bigi, J. H. Kühn, H. Schneider, Preprint MPI-PAE/PTh 28/78 (1978).
[2] N. Isgur, *Phys. Rev.* **D11**, 3236 (1975); R. Koniuk, R. Leroux, N. Isgur, *Phys. Rev.* **D17**, 2915 (1978).
[3] R. Budny, *Phys. Rev.* **D20**, 2763 (1979).
[4] For a textbook discussion, see e.g., J. J. Sakurai, *Invariance Principles and Elementary Particles*, Princeton University Press, Princeton, N. J., 1964.
[5] J. Bernabéu, P. Pascual, *Nucl. Phys.* **B173**, 93 (1980); τ decays as means to measure the lepton's helicity in $e^+e^- \to \tau^+\tau^-$ off resonance have been proposed also by H. Dahmen, L. Schülke, G. Zech, *Phys. Lett.* **81B**, 361 (1980); applications to Z_0-physics are discussed in the article by J. E. Augustin, Preprint ECFA/LEP 29 (1978).

Chapter III

[1] J. Kaplan, J. H. Kühn, *Phys. Lett.* **78B**, 252 (1978),
[2] B. Guberina, J. H. Kühn, R. D. Peccei, R. Rückl, *Nucl. Phys.* **B174**, 317 (1980).
[3] R. Barbieri, R. Gatto, R. Kögeler, *Phys. Lett.* **60B**, 183 (1976).
[4] A. Khare, *Nucl. Phys.* **B152**, 533 (1979).
[5] J. H. Kühn, J. Kaplan, E. G. O. Safiani, *Nucl. Phys.* **B157**, 125 (1979).
[7] J. H. Kühn, Preprint MPI-PAE/PTh 29/79 (1979) and in "Proc. of the II Int. Symp. on Hadron Structure and Multiparticle Production", Kazimierz, May 1979.

[8] A. Martin, in "Proc. of the II Int. Symp. on Hadron Structure and Multiparticle Production", Kazimierz, May 1979.
[9] J. H. Kühn, *Phys. Lett.* **89B**, 385 (1979).
[10] J. H. Kühn, Preprint MPI-PAE/PTh 32/80 (1980).

Chapter IV

A number of authors have emphasized the possible importance of weak onium decays.

[1] J. Ellis, M. K. Gaillard, in "*Physics with Very High Energy e^+e^- Colliding Beams*", Preprint CERN 76–18 (1976).
[2] J. Bjorken, in "Proc. of 1977 Hamburg Conference".
[3] K. Fujikawa, *Prog. Theor. Phys.* **61**, 1186 (1979).
[4] G. Goggi, G. Penso, *Nucl. Phys.* **B165**, 429 (1980).
[5] I. Bigi, H. Krasemann, Preprint TH2854-CERN (1980).
[6] J. Ellis, Preprint TH2910-CERN (1980).
[7] J. Rich, R. D. Winn, *Phys. Rev.* **D14**, 1283 (1976).
[8] T. M. Renard, *Z. Phys.* **C1**, 225 (1979).
[9] F. A. Wilczek, *Phys. Rev. Lett.* **39**, 1304 (1977).
[10] H. E. Haber, G. L. Kane, T. Sterling, Michigan Preprint UM-HE 78–45 (1978).
[11] M. Bander, A. Soni, UC Irvine Preprint 78–59 (1978).

Chapter V

[1] M. A. Bouchiat, C. Bouchiat, *Phys. Lett.* **48B**, 111 (1974).
[2] For a review see the article of P. G. H. Sanders in "Proc. of the 1977 Hamburg Conference".

Chapter VI

[1] H. Fritzsch, *Phys. Lett* **86B**, 164 (1979).
[2] J. H. Kühn, S. Nussinov, R. Rückl, *Z. Phys. C, Particles and Fields* **5**, 117 (1980). Results for ψ and ψ' only were independently obtined by M. B. Wise, Preprint Slac-PUB-2399 (1979), and for ψ and η_c by T. A. DeGrand and D. Toussaint, UCSB Preprint TH-18 (1979).
[3] M. K. Gaillard, B. W. Lee, *Phys. Rev. Lett.* **33**, 108 (1974); G. Altarelli, L. Maiani, *Phys. Lett.* **52B**, 351 (1974).

Chapter VII

[1] C. A. Piketty, L. Stodolsky, *Nucl. Phys.* **B15**, 511 (1970).
[2] M. K. Gaillard, S. A. Jackson, D. V. Nanopoulos, *Nucl. Phys.* **B102**, 326 (1976).
[3] A. Bartl, H. Fraas, W. Majerotto, *Phys. Rev.* **D16**, 2124 (1977).
[4] J. H. Kühn, R. Rückl, *Phys. Lett.* **95B**, 431 (1980).
[5] V. Barger, W. Y. Keung, R. J. N. Phillips, Preprint COO-881-128 (1980).
[6] H. Fritsch, *Phys. Lett* **67B**, 217 (1977).
[7] T. Nash et al., *Phys. Rev. Lett.* **36**, 1233 (1976), and references to earlier photo-production data therein.
[8] A. R. Clark et al., *Phys. Rev. Lett.* **43**, 187 (1979), LBL Preprints LBL-10747 (April 1980), LBL-10879 (May 1980) and LBL-11009 (June 1980).
[9] J. J. Aubert et al., *Phys. Lett.* **89B**, 267 (1980), CERN Preprint CERN-EP/80–84 (June 1980).
[10] H. Fritzsch, K. H. Streng, *Phys. Lett.* **72B**, 385 (1978).
[11] M. Glück, E. Reya, *Phys. Lett.* **79B**, 453 (1978), **83B**, 98 (1979).
[12] J. P. Leveille, T. Weiler, *Nucl. Phys.* **B147**, 147 (1979), *Phys. Lett.* **86B**, 377 (1979); T. Weiler, *Phys. Rev. Lett.* **44**, 304 (1980).
[13] V. Barger, W. Y. Keung, R. J. N. Phillips, *Phys. Rev.* **D20**, 630 (1979), *Phys. Lett.* **91B**, 253 (1980), **92B**, 179 (1980).
[14] K. Kleinknecht, Talk given at the DPG-meeting, Dortmund, February 27–29, 1980.